



Imaging system based on silicon photomultipliers and light emitting diodes for functional near-infrared spectroscopy

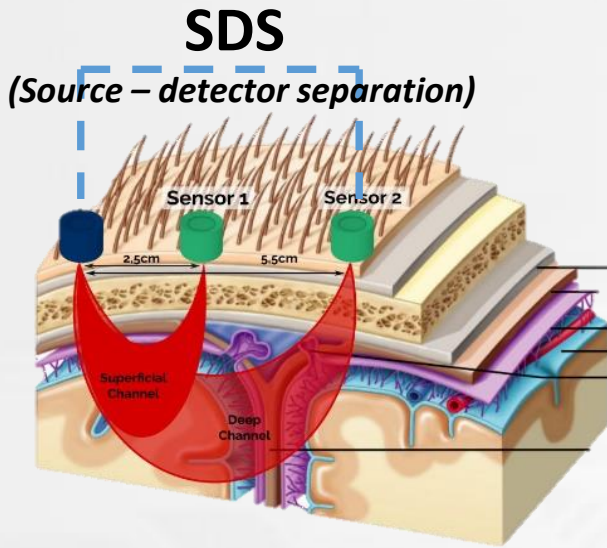
Giovanni Maira ^{1,*}, *Antonio M. Chiarelli* ², *Stefano Brafa* ³, *Sebania Libertino* ¹, *Giorgio Fallica* ⁴,
Arcangelo Merla ² and *Salvatore Lombardo* ¹

1. IMM-CNR, Catania
2. Department of Neuroscience, Imaging and Clinical Sciences University G. D'Annunzio of Chieti – Pescara
3. Department of Electrical Electronic and Computer Engineering, University of Catania
4. STMicroelectronics (Catania)

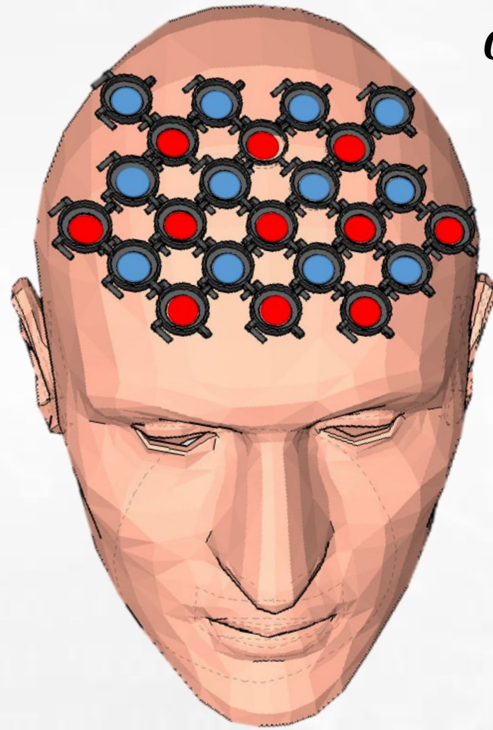
* Now at STMicroelectronics (Catania)

CW - functional Near Infrared Spectroscopy

Scattering + Absorption
in a «semitransparent tissue»

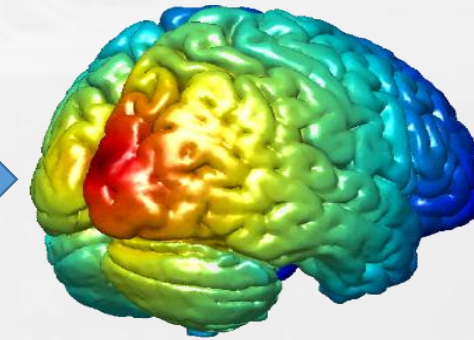
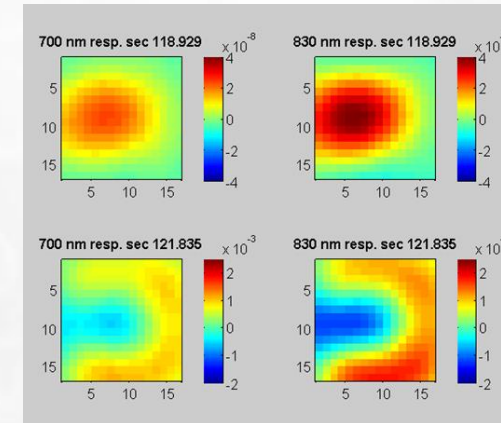
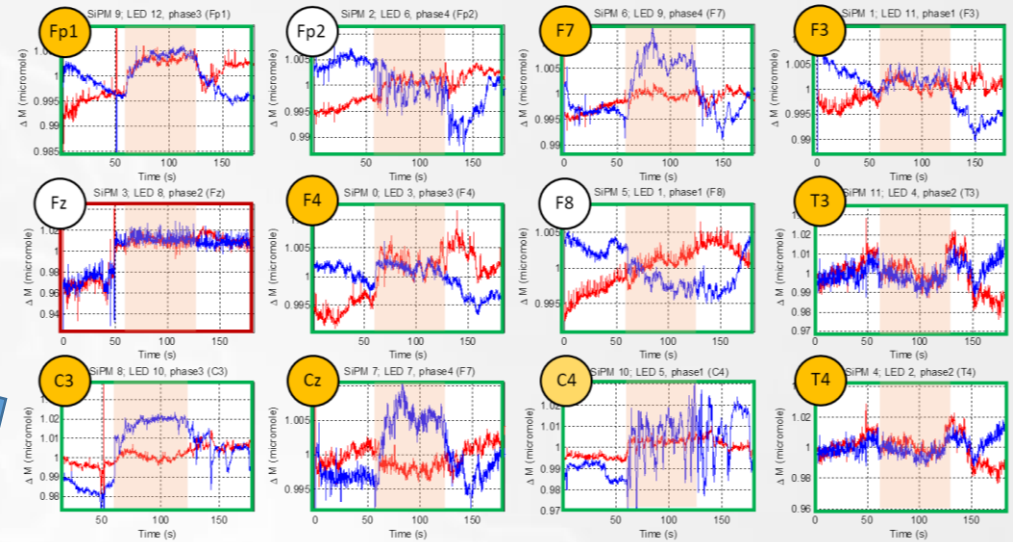


1 channel



N channels
(time division)

$O_2Hb(t)$
 $HHb(t)$



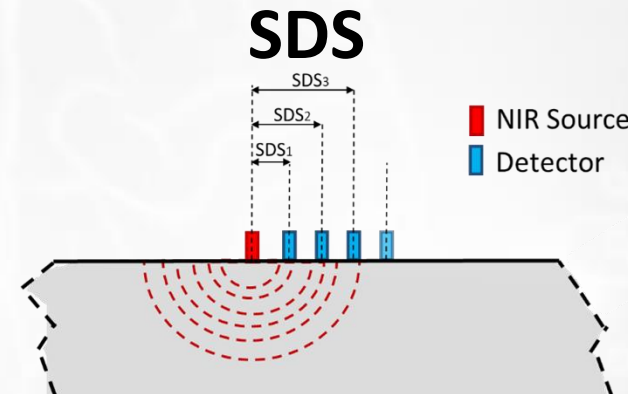
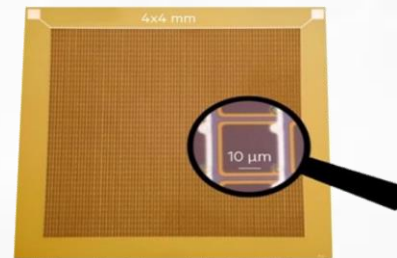
Topics and Objectives

Identify a class of
Solid State photodetectors
with **improved responsivity** in
order to detect weak optical signals



Silicon Photomultipliers

- right typology
- suitable operation conditions



Knowledge of
Light Scattering in
diffusive media



Optical Phantoms

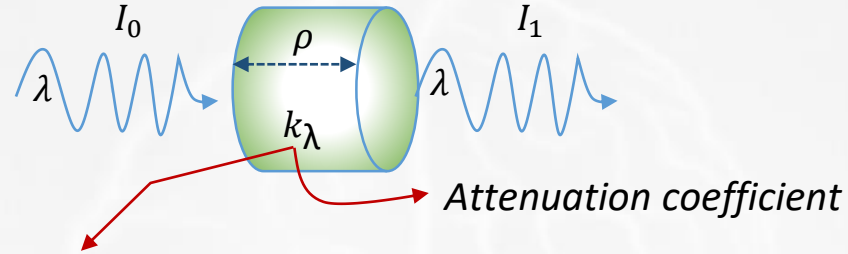
- Modeling
- Measurements

- number of channels (spatial resolution) 
- depth 

General Context: functional Near Infrared Spectroscopy

modified Beer-Lambert Law

$$\frac{I_1}{I_0} = e^{-\rho \cdot k_\lambda}$$



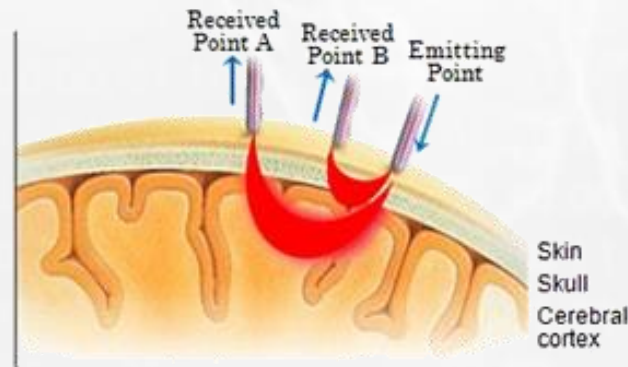
In a solution with 2 species: $k_\lambda \rightarrow \epsilon_1 \cdot M_1 + \epsilon_2 \cdot M_2$

«banana shape» \Rightarrow «differential pathlength factor» $DPF(\lambda)$

$$M(t) = - \frac{1}{\rho \cdot \epsilon_\lambda \cdot DPF(\lambda)} \ln \left[\frac{I(t)}{I_0} \right] (*)$$

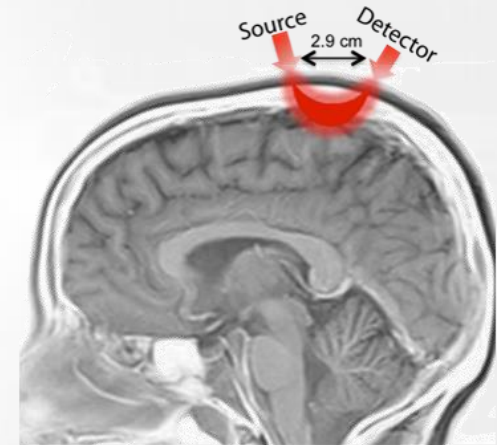
Optical Density

$$OD = - \ln \left[\frac{I(t)}{I_0} \right]$$



Rule of thumb:
Max sensitivity
at SDS/2

SDS

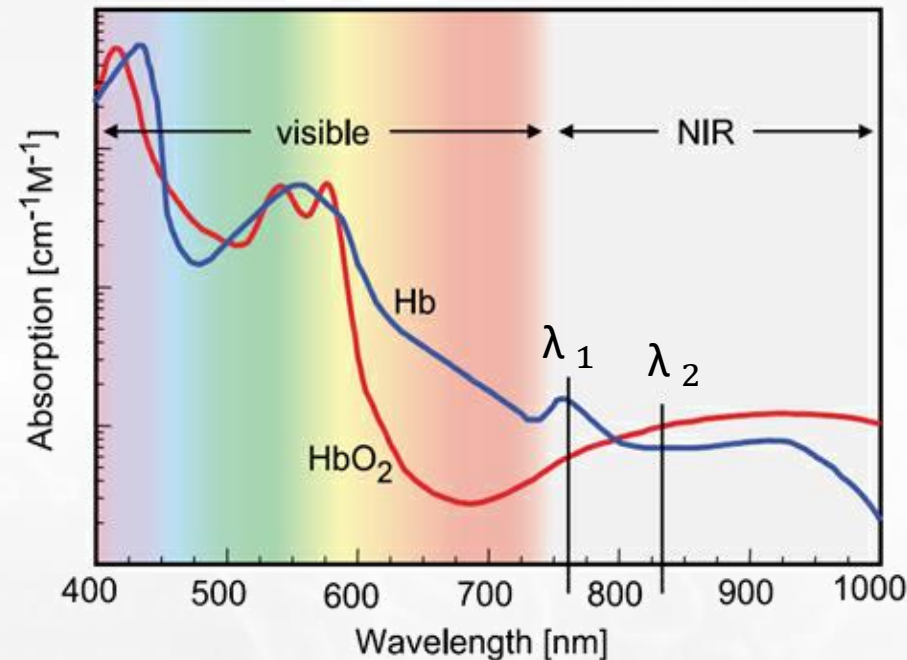


* Felix Scholkmann and Martin Wolf, General equation for the differential pathlength factor of the frontal human head depending on wavelength and age, Journal of Biomedical Optics 18(10), 105004 (October 2013)

functional Near Infrared Spectroscopy

O₂Hb and HHb, modified Beer-Lambert Law

$$\begin{bmatrix} O_2Hb(t) \\ HHb(t) \end{bmatrix} = \frac{1}{\rho} \begin{bmatrix} \varepsilon_{O_2Hb}(\lambda_1) \cdot DPF(\lambda_1) & \varepsilon_{HHb}(\lambda_1) \cdot DPF(\lambda_1) \\ \varepsilon_{O_2Hb}(\lambda_2) \cdot DPF(\lambda_2) & \varepsilon_{HHb}(\lambda_2) \cdot DPF(\lambda_2) \end{bmatrix}^{-1} \begin{bmatrix} OD(\lambda_1, t) \\ OD(\lambda_2, t) \end{bmatrix}$$



$$\varepsilon_{O_2Hb}(700 \text{ nm}) = 9 \times 10^{-5} \text{ mm}^{-1}$$

$$\varepsilon_{HHb}(700 \text{ nm}) = 4.4 \times 10^{-4} \text{ mm}^{-1}$$

$$\varepsilon_{O_2Hb}(830 \text{ nm}) = 2.4 \times 10^{-4} \text{ mm}^{-1}$$

$$\varepsilon_{HHb}(830 \text{ nm}) = 1.9 \times 10^{-4} \text{ mm}^{-1}$$

By choosing 2 different wavelengths near the **isobestic point** (the first lower and the second greater), it is possible to calculate the variation of the two molecular concentrations.

CW - fNIRS State of the Art

Measured Parameters: EROS	<ul style="list-style-type: none"> • Signal intensity • Signal phase delay
Light Sources:	<ul style="list-style-type: none"> • <u>Fiber coupled laser diodes</u> • <u>Wavelengths: 690 nm and 830 nm</u> • <u>Laser power: 10 mW average</u>
Light Detectors:	<ul style="list-style-type: none"> • <u>Photomultiplier tubes</u>
Optodes:	<ul style="list-style-type: none"> • <u>Paired fibers in excitation, 400µm diameter</u> • <u>Fiber bundle in collection, 3mm diameter</u>



ImagentTM
Functional Brain Imaging System
Using Infrared Photons

(2016)

Photomultiplier tubes
with fibers as probe

Intrinsic Gain: 10^7 electrons per detected photon

- (1) Wearable design with compact capsule and no optical fibers
- (2) High sensitivity by APDs (linear mode)
- (3) Support multi-distance measurement mode
- (4) LED for checking sensor fitting status



HITACHI
Inspire the Next

(2016)

Avalanche photodiodes
directly placed on the scalp

Intrinsic Gain: 10^2 electrons per detected photon

Number of Detector Channels	8
Sensitivity	< 1pW
Dynamic Range	60 dBopt
Sensor Type	<u>Si Photodiode, Active Sensor</u>
Number of Illumination Sources	8 (Time-Multiplexed)
Source Wavelengths, Emitter Type	<u>760nm & 850nm LED</u>



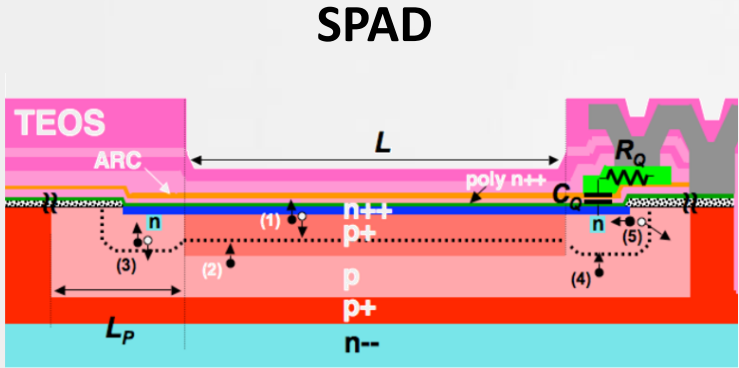
NIRX

(2018)

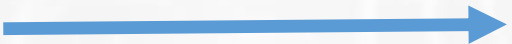
Silicon Photodiodes
directly placed on the scalp

Intrinsic Gain: **1** electron per detected photon

Solid State photodetectors: Silicon Photomultipliers

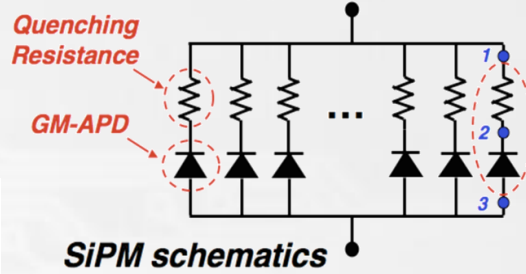
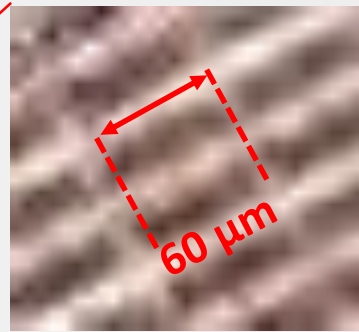
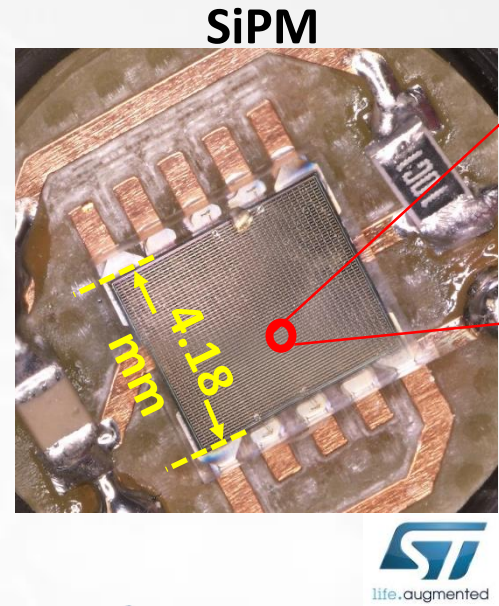


Photomultiplier Tubes (PMTs) for scintillators:

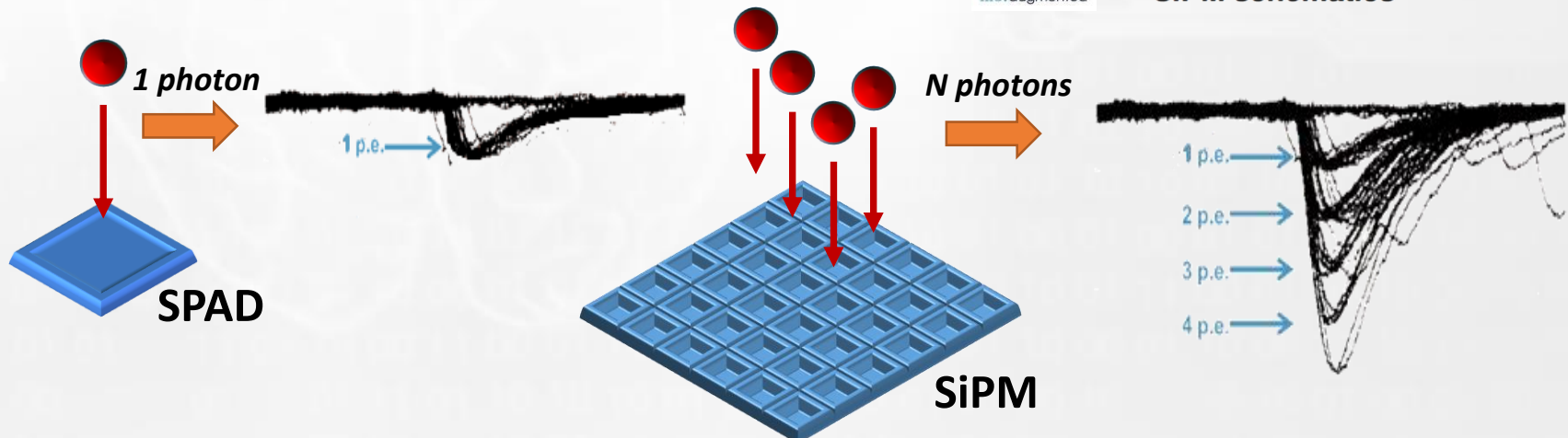
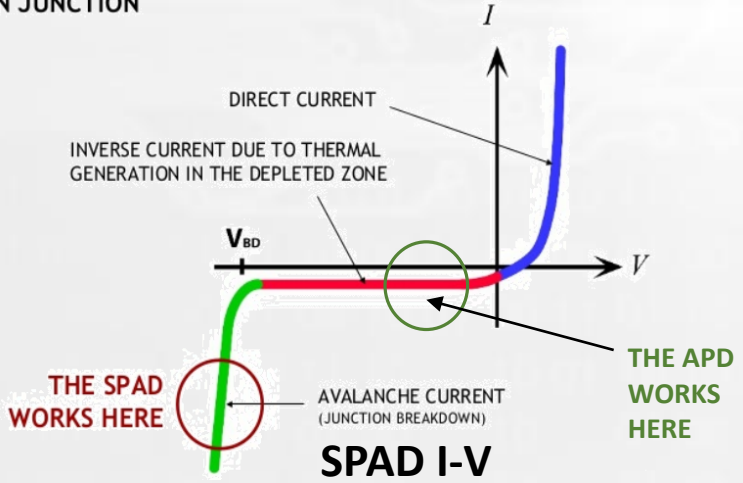


LARGE AREA
High Responsivity

bi-dimensional array of SPADs

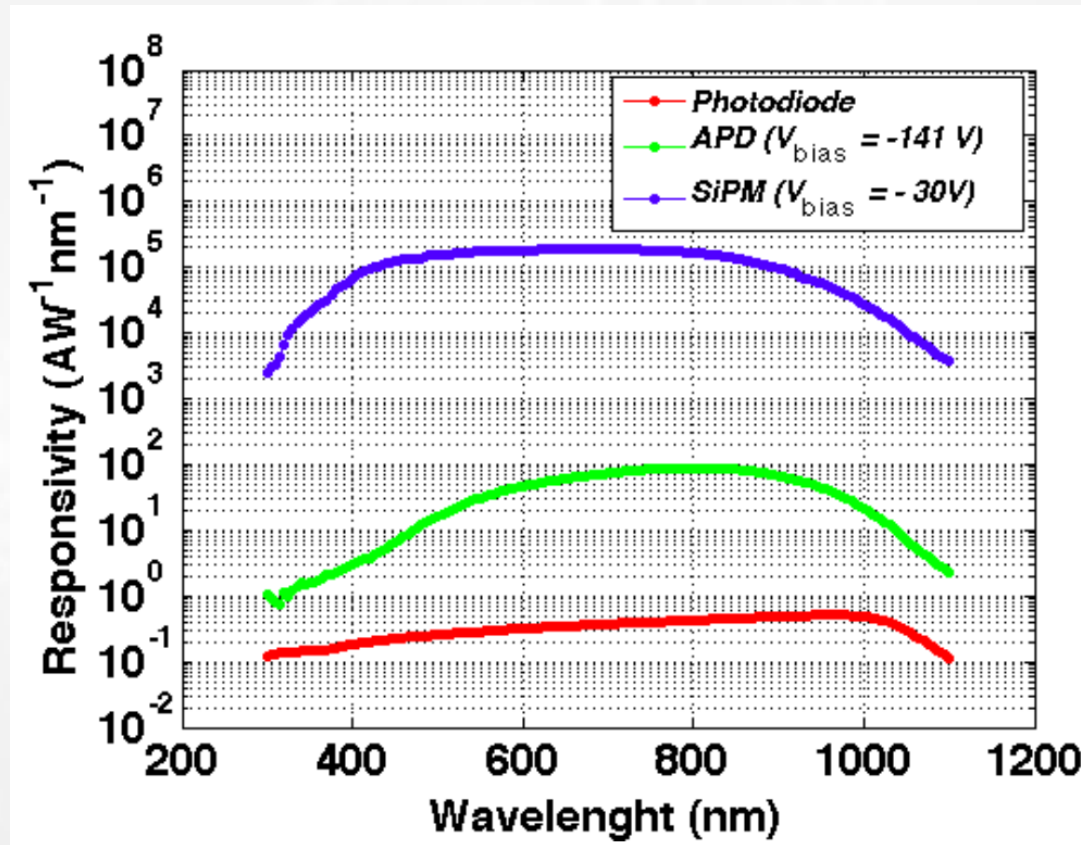


Geiger mode:
gain $10^6 \div 10^7$
N JUNCTION



Solid State photodetectors: Silicon Photomultipliers

SiPM responsivity:
Comparable to PMT responsivity
(orders of magnitude higher than APDs and PDs)



Responsivity: output signal / optical power impinging the detector.

The In-Vivo Stimulus (N on P SiPM)

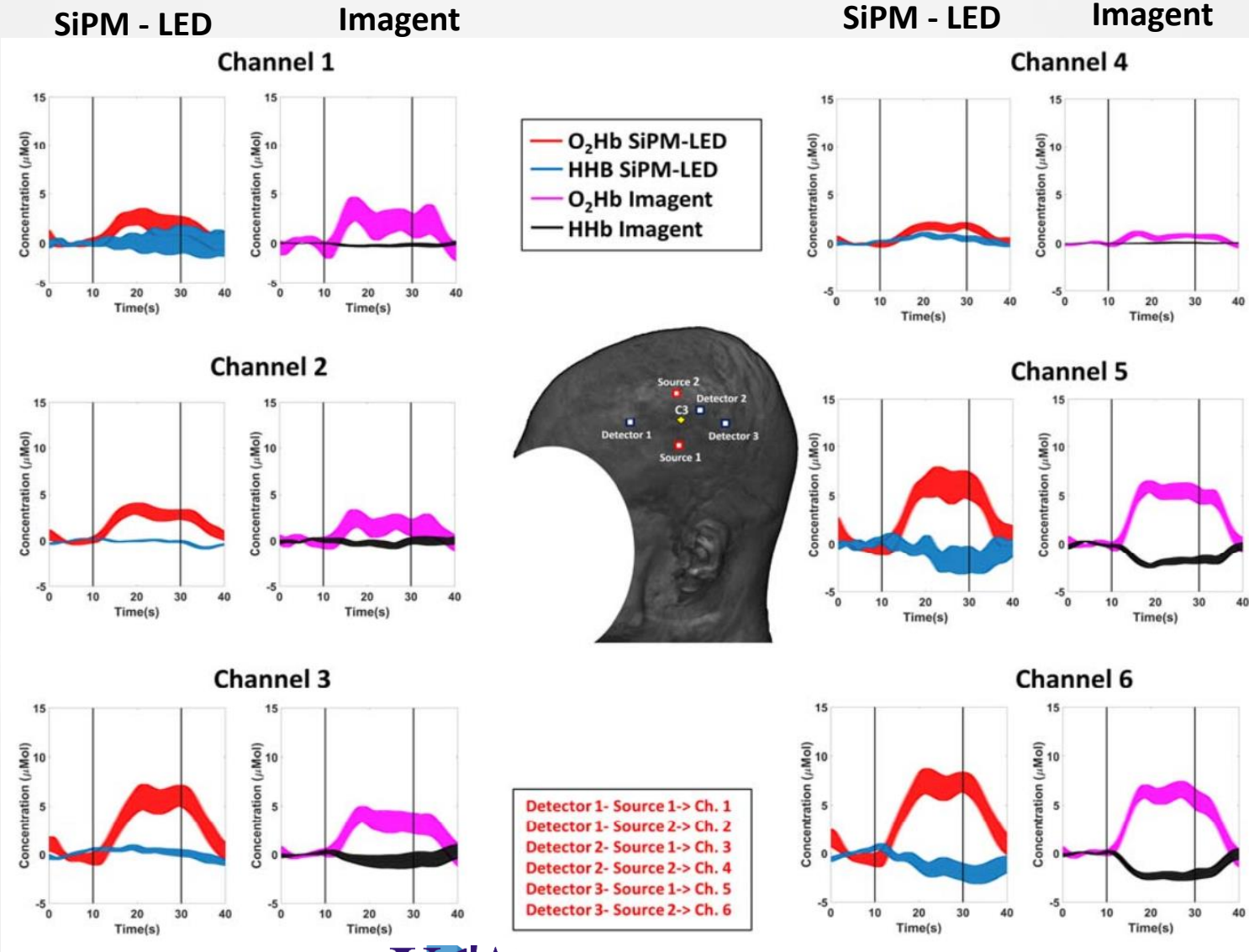
off-line

Sensors located in **C3** location (based on the 10-20 system for EEG)
 Subject right-handed in sitting comfortably on a chair

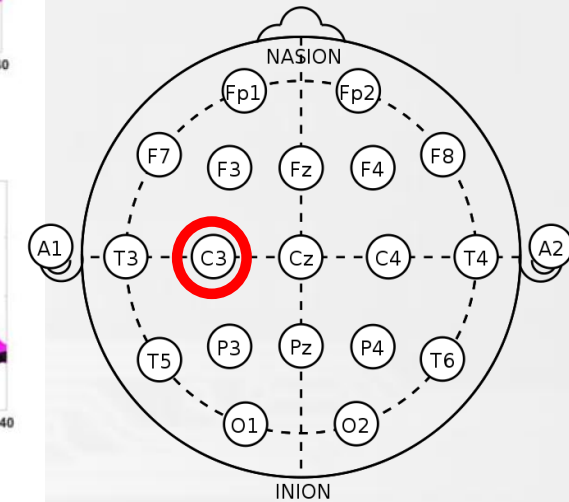
Right-hand finger tapping task locked to an auditory stimulation ('start', 'stop' commands),

4 consecutive runs. One run: **40** seconds of rest, **20** seconds' task and **20** seconds rest X 4 times
Total of 16 finger tapings

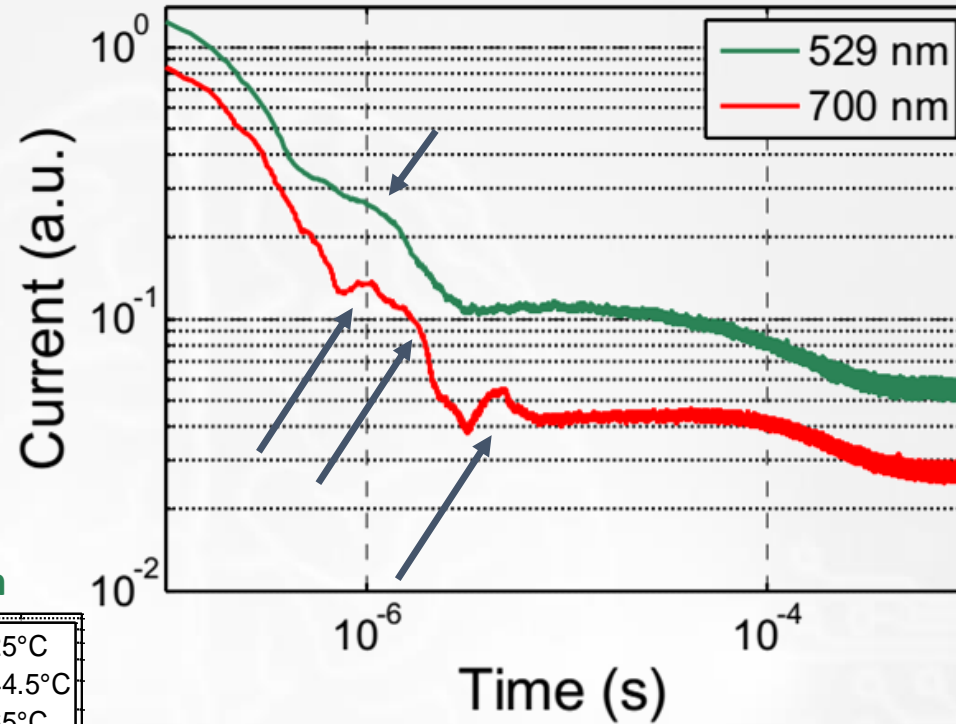
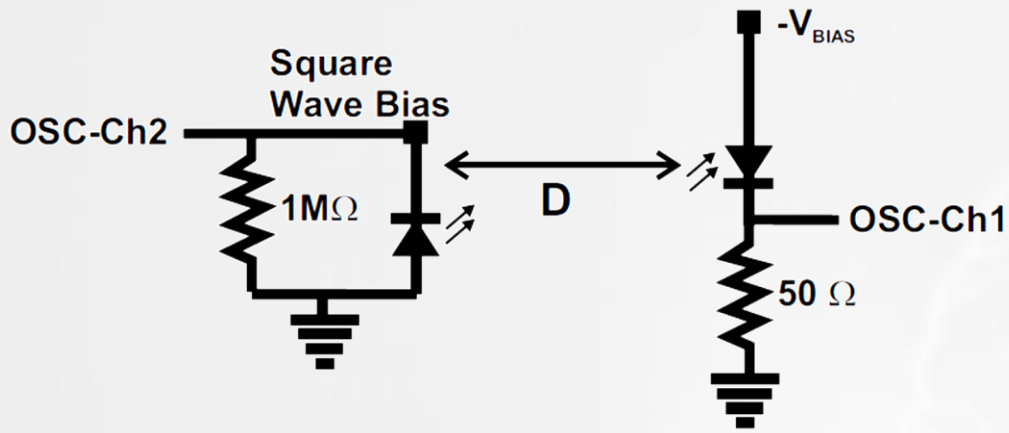
Same procedure for the two systems.



10-20 system for EEG



SiPM characterization: Afterpulsing



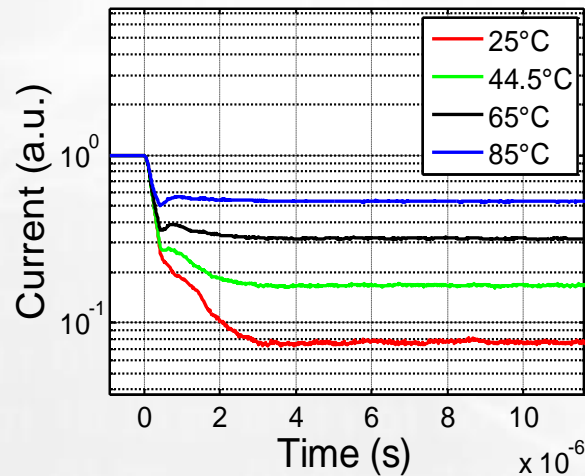
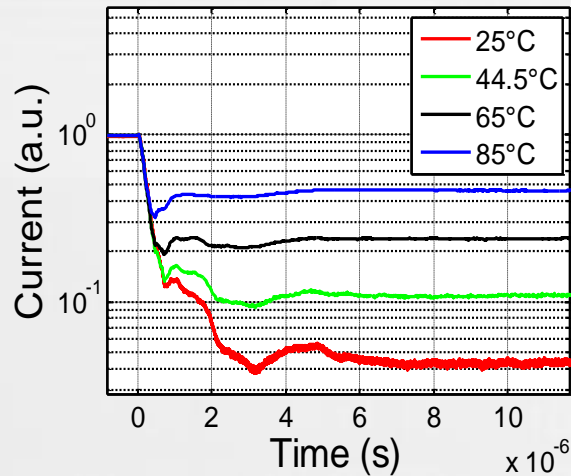
The absorption coefficient (α) is $\sim 3 \times 10^3$ and $\sim 8 \times 10^2 \text{ cm}^{-1}$ at 529 and 700 nm, corresponding to absorption lengths of ~ 3.3 and $\sim 12.5 \mu\text{m}$, respectively. Since 95% of the light is absorbed within a $3/\alpha$ thickness, we estimate that the “illuminated” region, i.e. the detector absorption region, is about **10 μm** and **37.5 μm** at 529 nm and 700 nm, respectively

At 700 nm the peaks are at $t = 1; 1.5; 4.5 \mu\text{s}$, which correspond to depths estimated as $\sqrt{(D * t)/3}$ ($D = 12 \text{ cm}^2/\text{s}$) is the hole diffusivity, of **20, 25, and 43 μm**

SiPM transient after 529 nm (green) and 735 nm (red) wavelength LED switch-off, averaged on **500 traces at 100 MHz** sampling frequency

(a) 700 nm

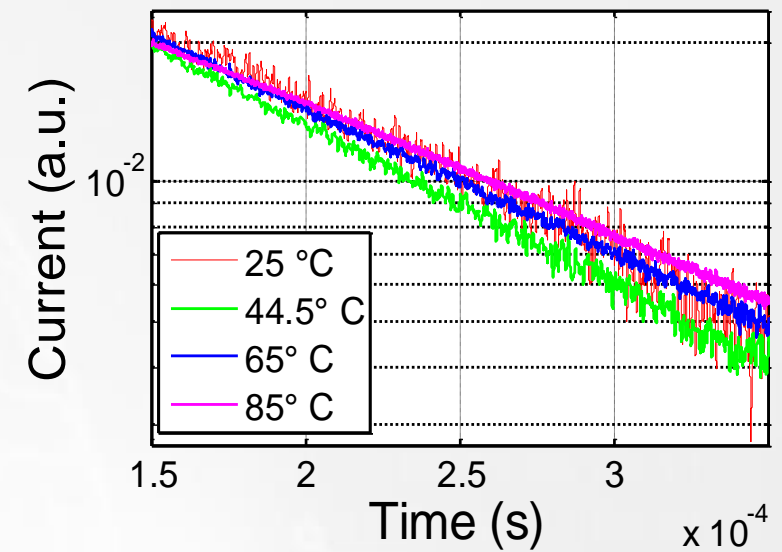
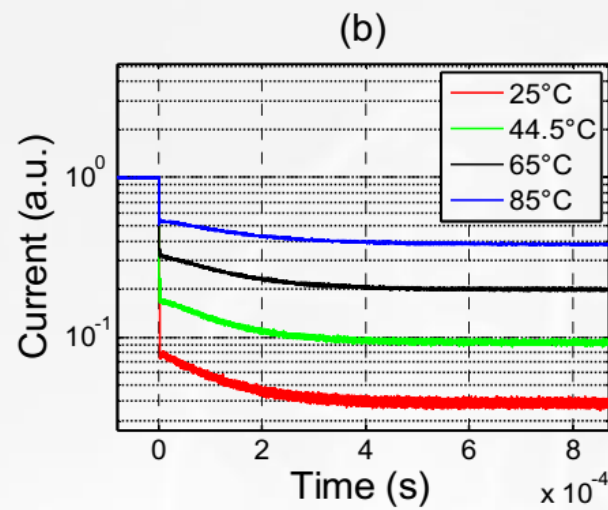
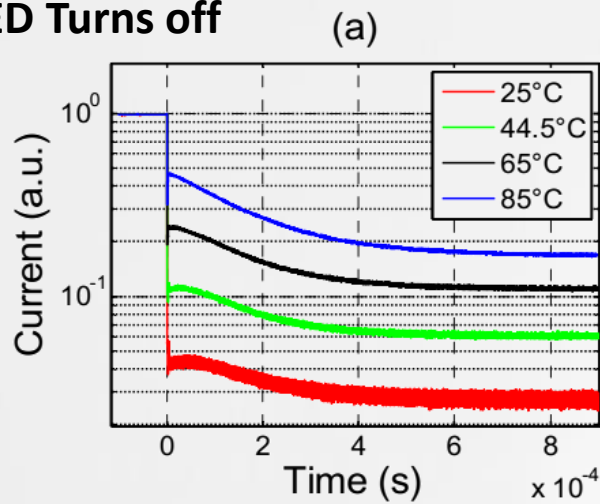
(b) 529 nm



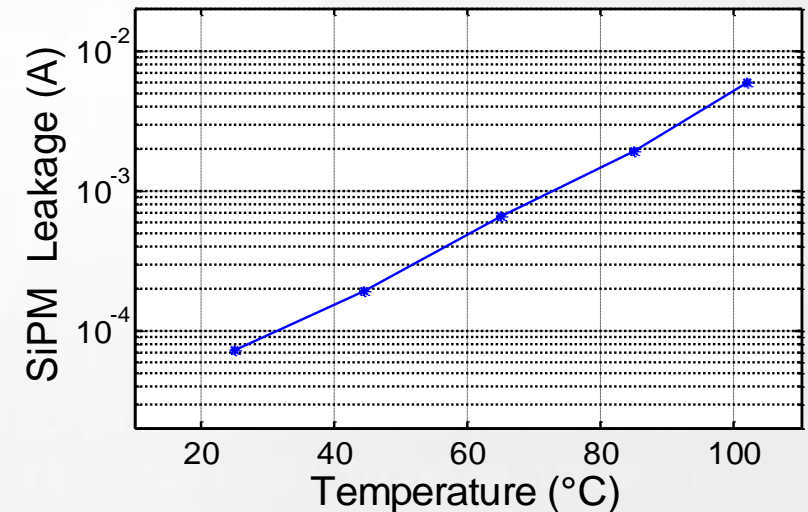
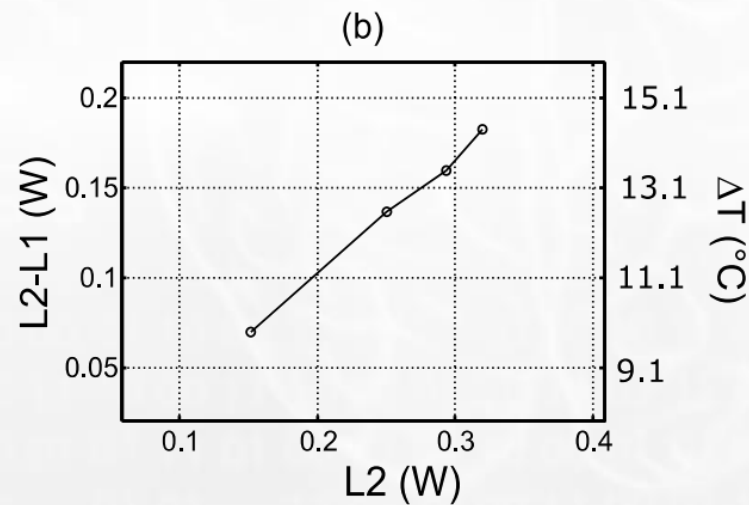
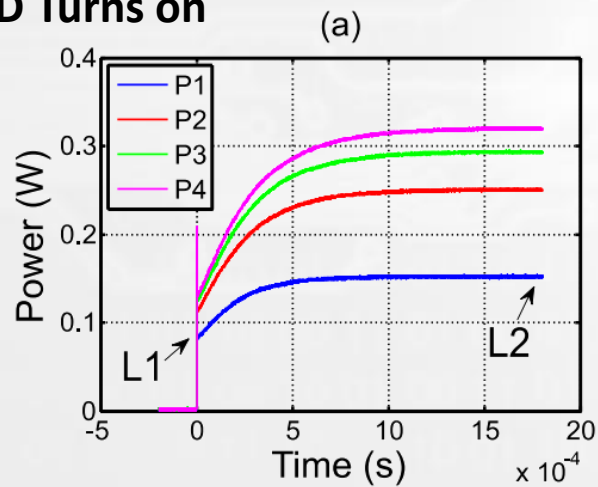
G. Maira, M. Mazzillo, S. Libertino, G. Fallica, S. Lombardo, «Crucial Aspects for the use of Silicon Photomultiplier devices in continuous wave functional near-infrared Spectroscopy», Biomedical Optics Express (2018)

SiPM characterization: Transients

LED Turns off



LED Turns on



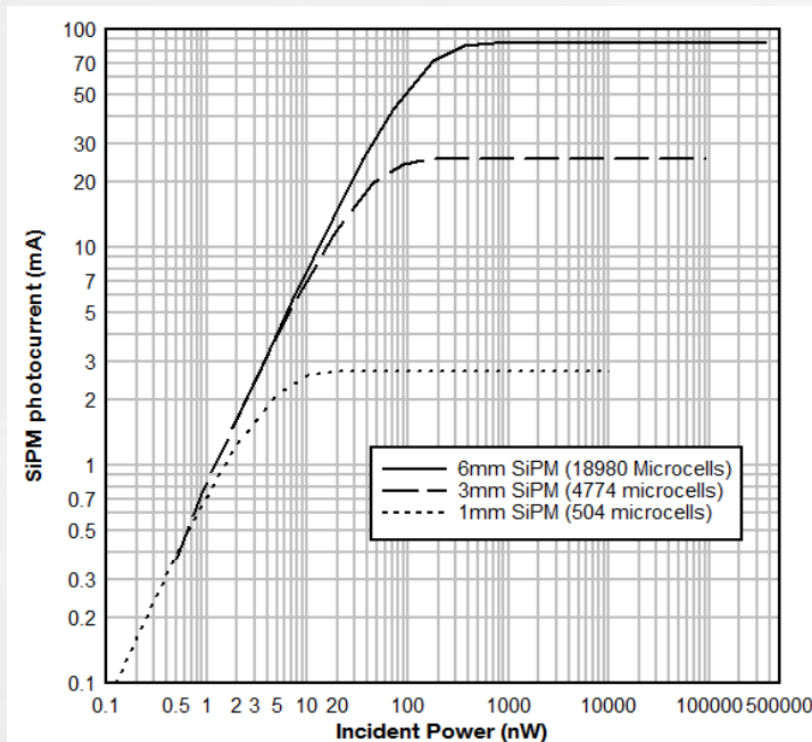
G. Maira, M. Mazzillo, S. Libertino, G. Fallica, S. Lombardo, «Crucial Aspects for the use of Silicon Photomultiplier devices in continuous wave functional near-infrared Spectroscopy», Biomedical Optics Express (2018)

SiPM characterization: Linear Range

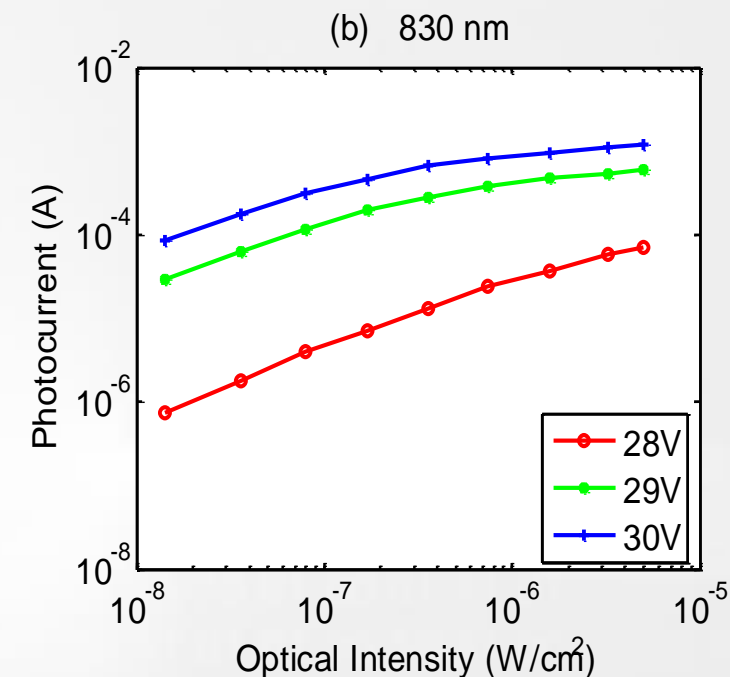
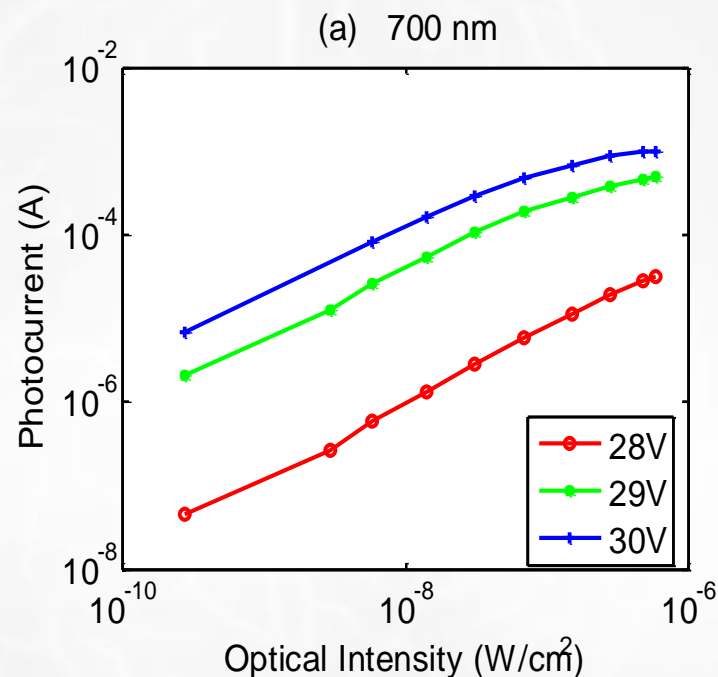
$$MAX = N_{pixel} / (EQE \cdot T_{quench})$$

$$MIN = 3dB + N_{pixel} / t_{dark}$$

Device



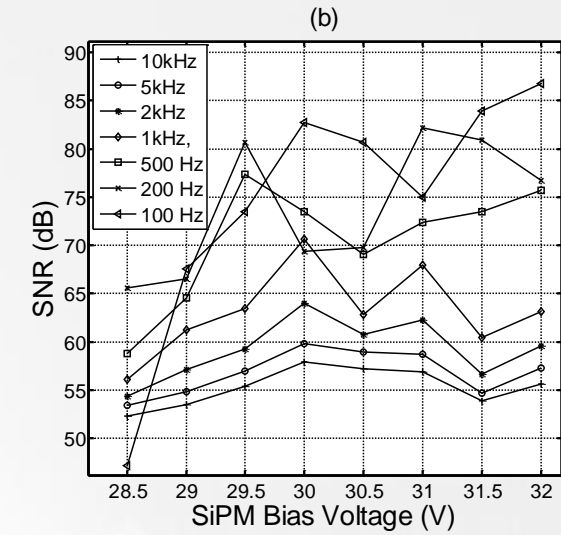
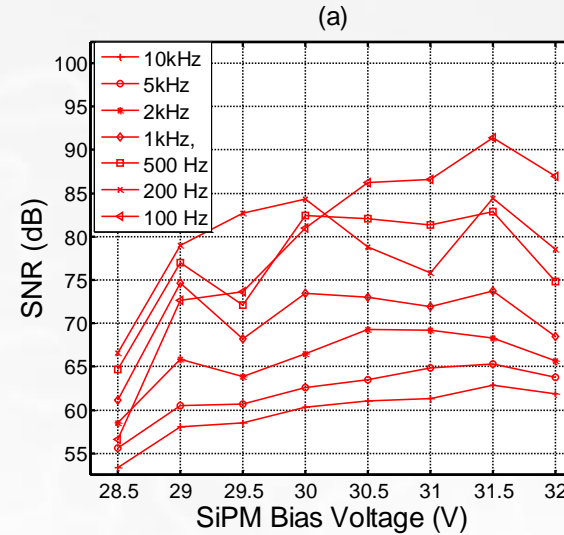
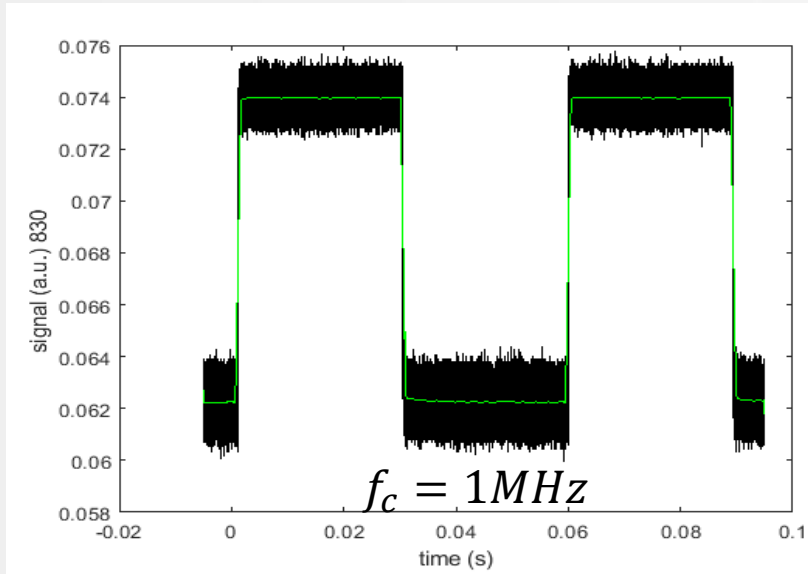
System channel



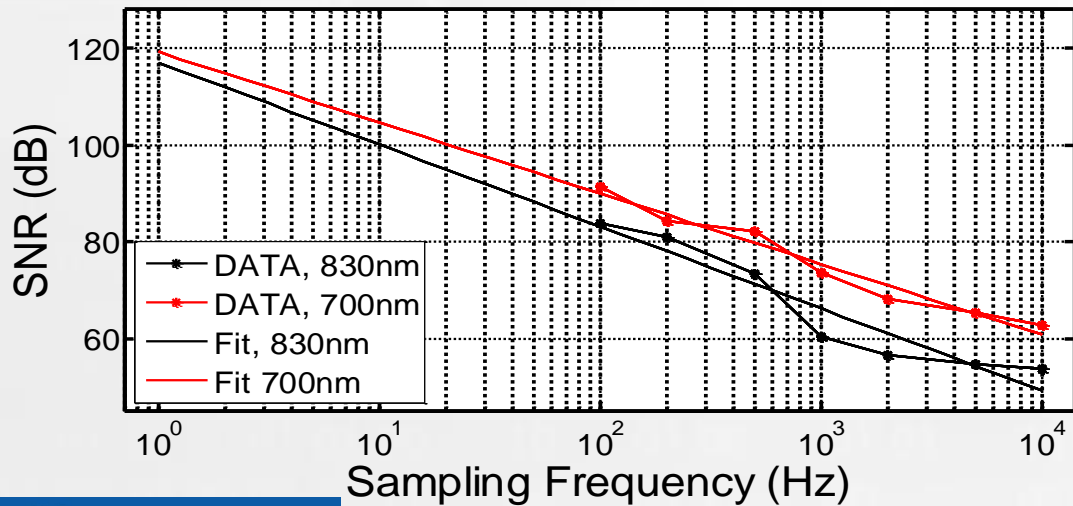
[Patent Application](#) of CNR and Ud'A, Authors list: **Giovanni A. Maira**, Salvatore A. Lombardo, Sebania Libertino, Arcangelo Merla, Antonio M. Chiarelli.

G. Maira, A.M. Chiarelli, S. Brafa, S. Libertino, G. Fallica, A. Merla, S. Lombardo «Imaging system based on Silicon Photomultipliers and Light Emitting diodes for functiona Near Infrared Spectroscopy», Applied Sciences (2020)

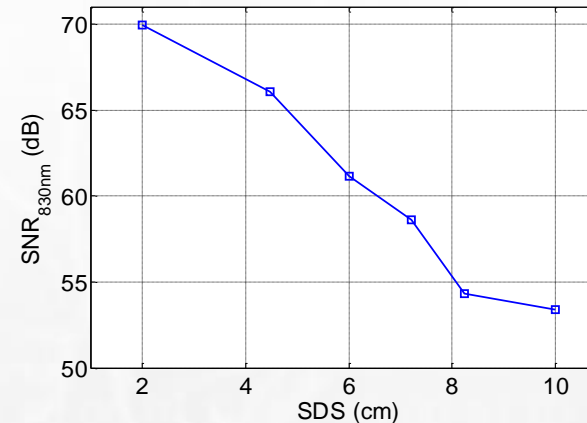
fNIRS System Signal to Noise Ratio



(c)



system SNR

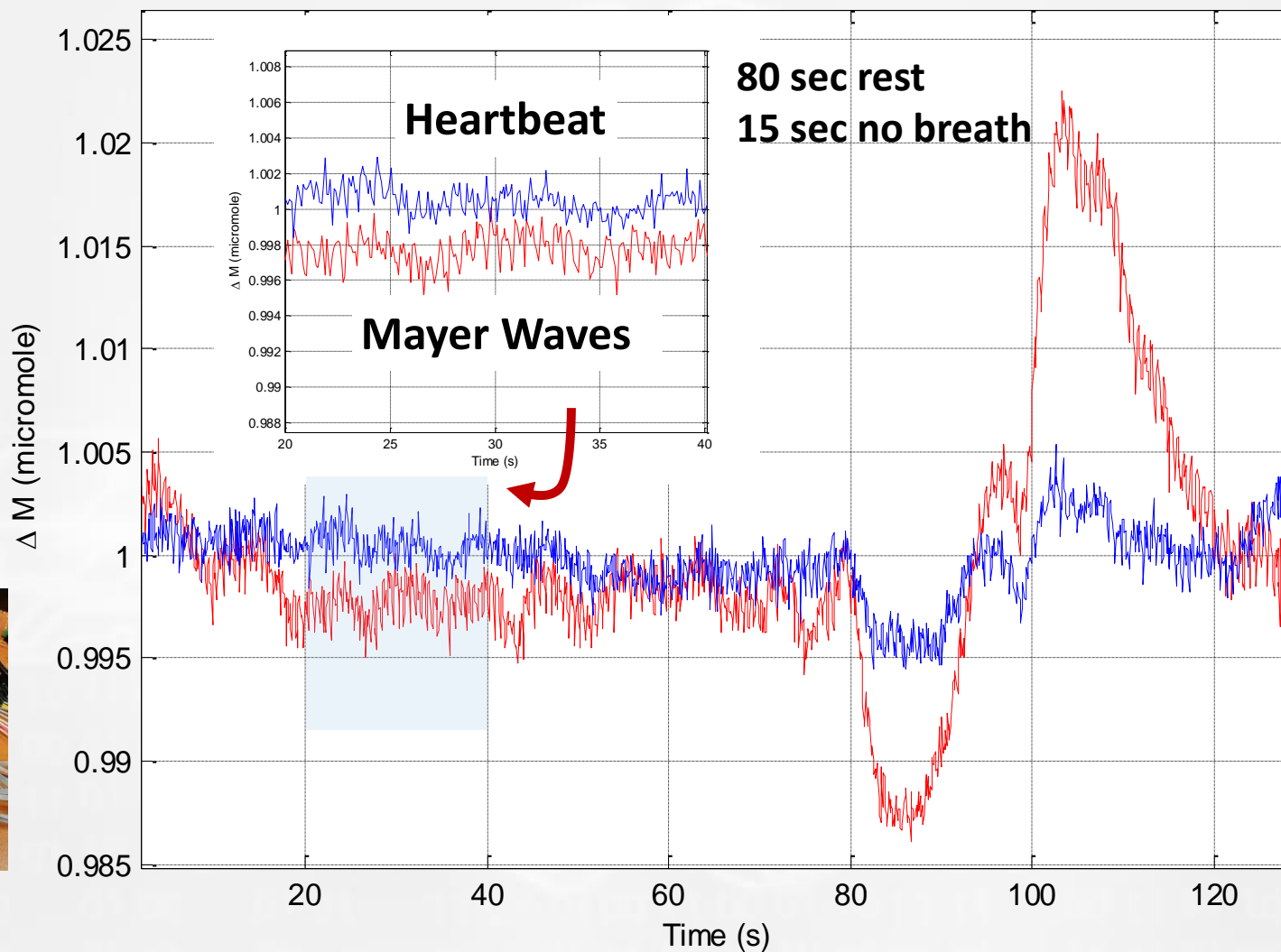


70 dB

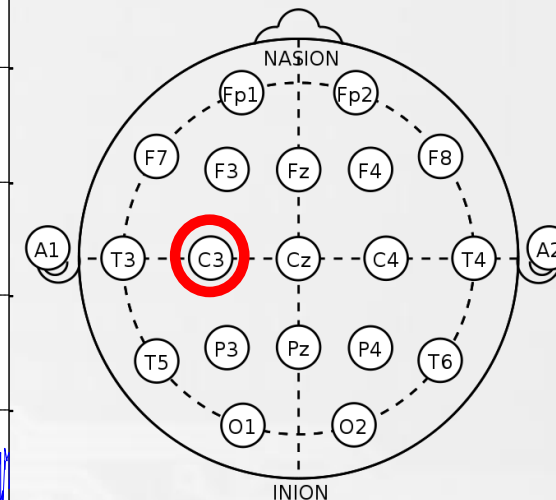
G. Maira, M. Mazzillo, S. Libertino, G. Fallica, S. Lombardo, «Crucial Aspects for the use of Silicon Photomultiplier devices in continuous wave functional near-infrared Spectroscopy», Biomedical Optics Express (2018)

G. Maira, A.M. Chiarelli, S. Brafa, S. Libertino, G. Fallica, A. Merla, S. Lombardo «Imaging system based on Silicon Photomultipliers and Light Emitting diodes for functional Near Infrared Spectroscopy», Applied Sciences (2020)

1 fNIRS channel: breath test



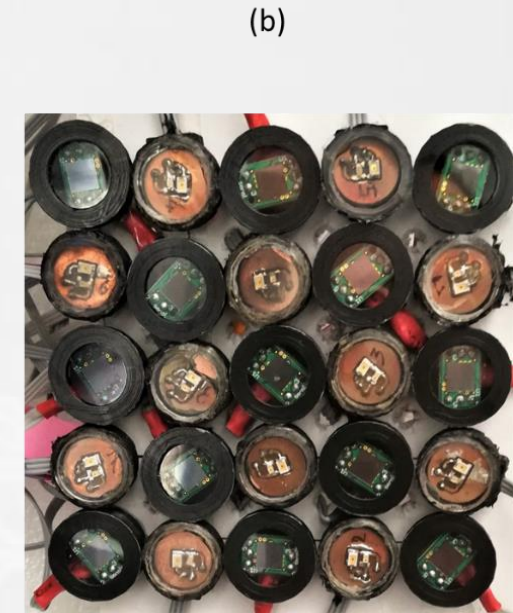
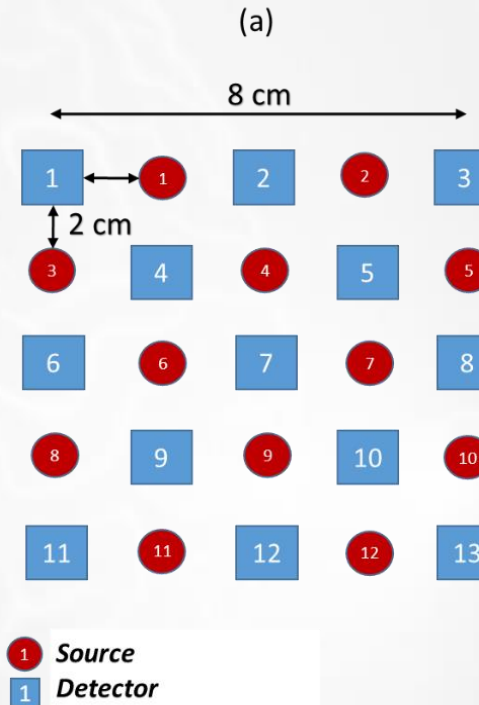
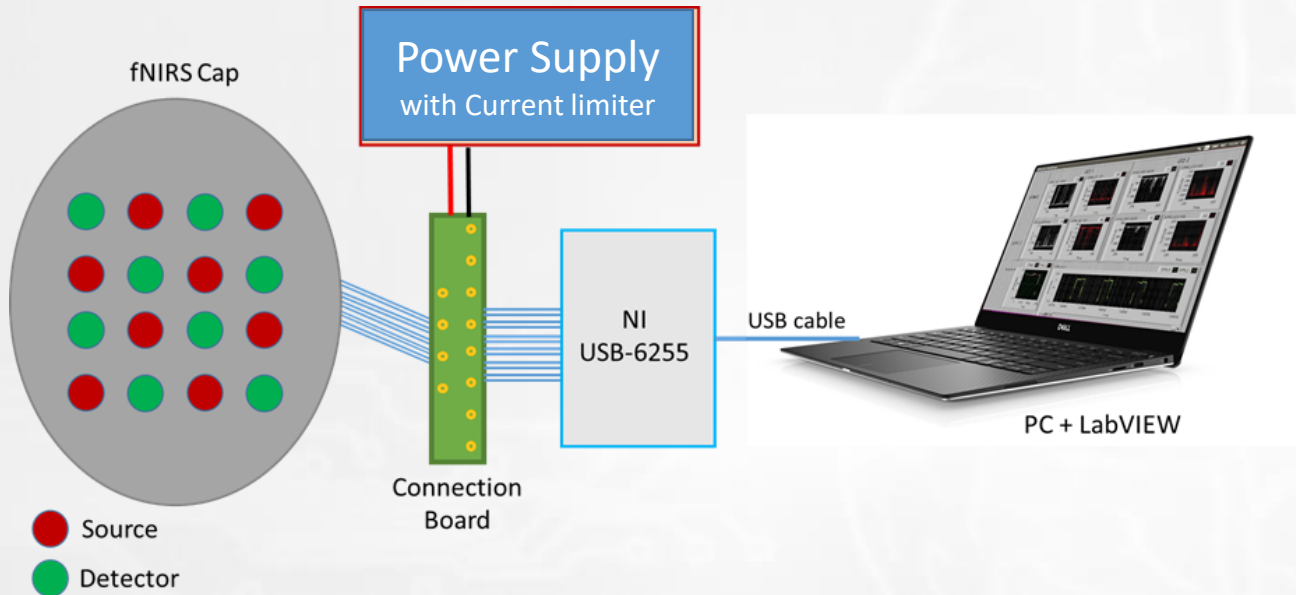
10-20 system for EEG



SDS = 3cm



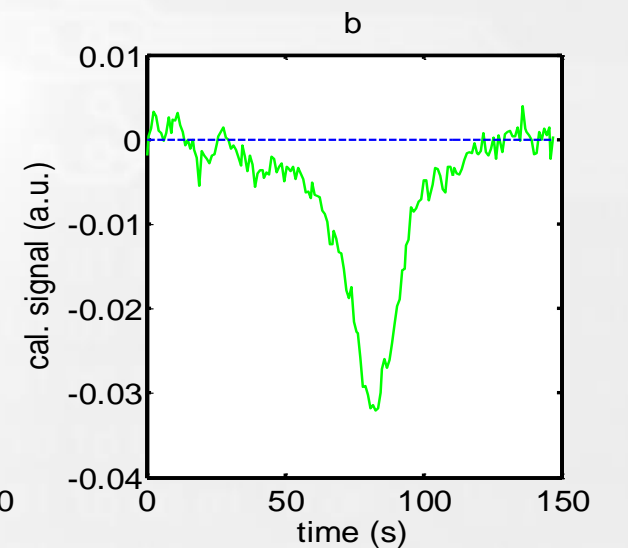
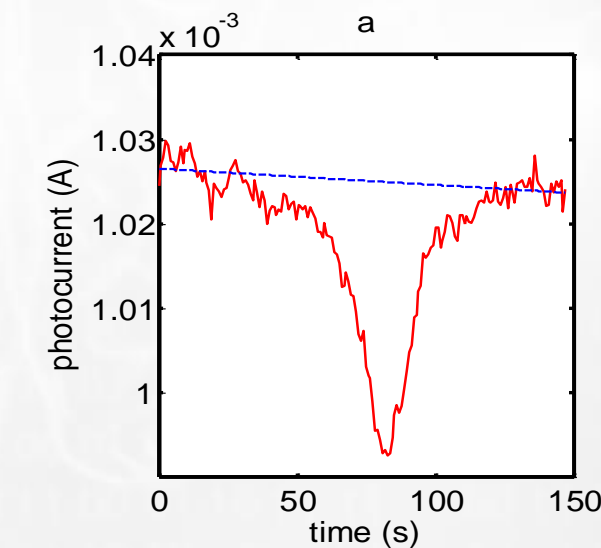
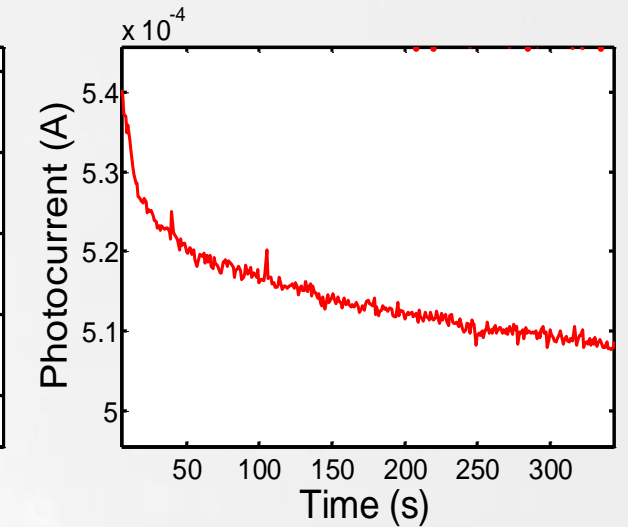
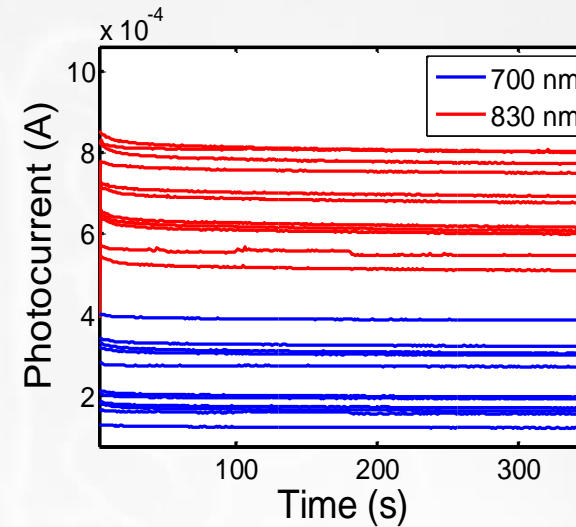
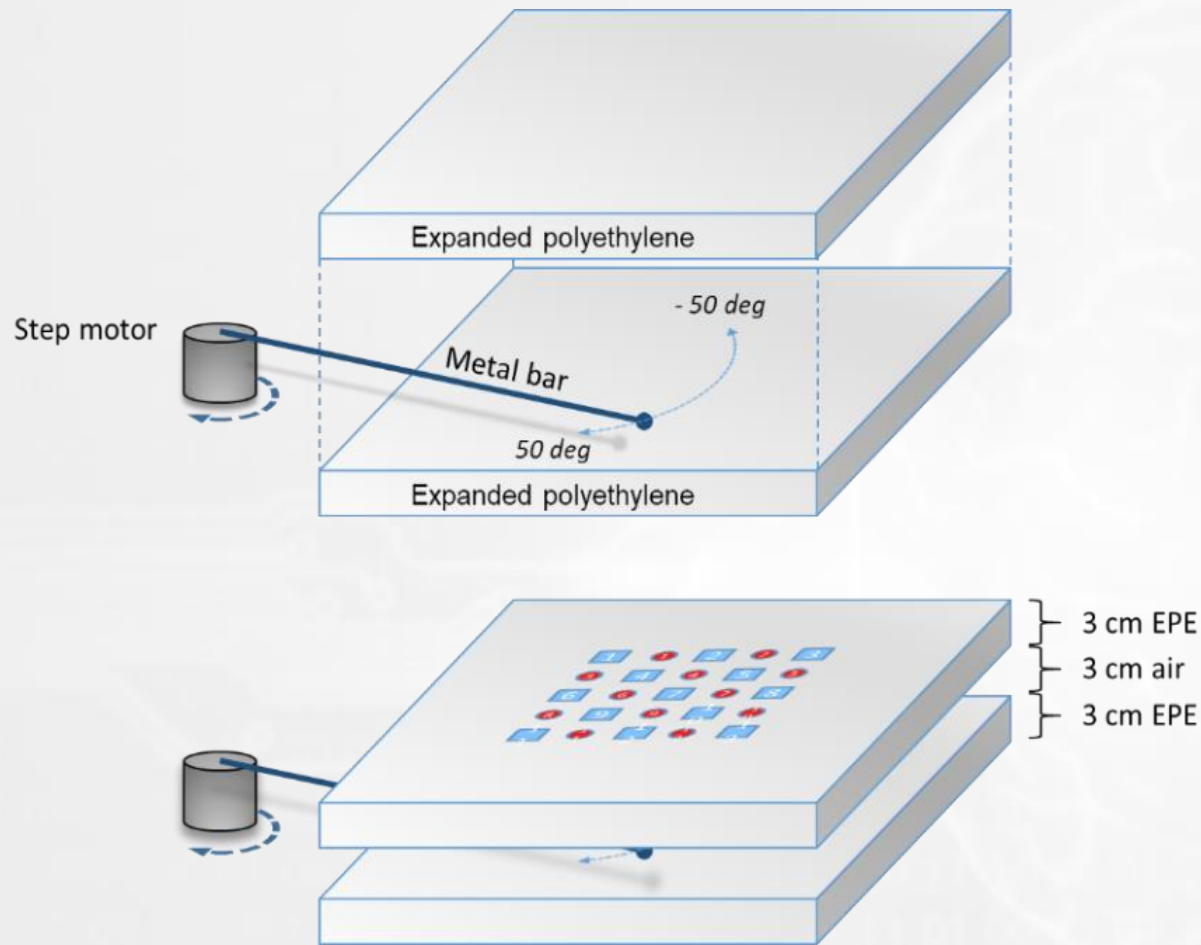
fNIRS / DOT (Diffuse Optical Tomography) multichannel prototype system



**156 channels,
2 wavelengths**

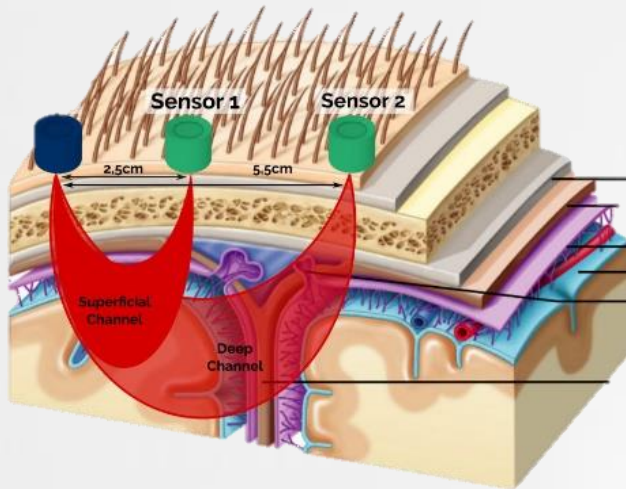
G. Maira, A.M. Chiarelli, S. Brafa, S. Libertino, G. Fallica, A. Merla, S. Lombardo «Imaging system based on Silicon Photomultipliers and Light Emitting diodes for functiona Near Infrared Spectroscopy», Applied Sciences (2020)

Dynamic Phantom and calibration algorithm



G. Maira, A.M. Chiarelli, S. Brafa, S. Libertino, G. Fallica, A. Merla, S. Lombardo «Imaging system based on Silicon Photomultipliers and Light Emitting diodes for functiona Near Infrared Spectroscopy», Applied Sciences (2020)

The Phantom



850 nm		
Tissue Type	μ_a (mm ⁻¹)	μ_s' (mm ⁻¹)
Scalp	0.012	1.8
Skull	0.025	1.6
Modified CSF	0.009	0.8
Gray Matter	0.036	0.9
White Matter	0.014	1.1

$$\mu_s' = 10 \text{ cm}^{-1}$$

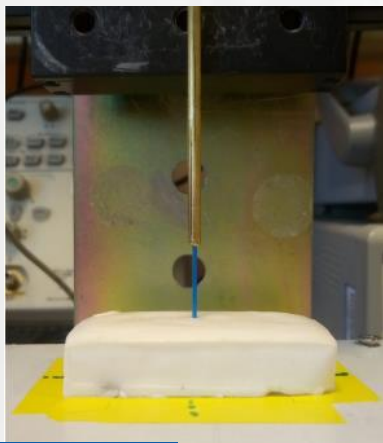
$$\mu_a = 0.1 \text{ cm}^{-1}$$

↓

$$\sqrt{\mu_a \cdot \mu_s'} = 1 \text{ cm}^{-1}$$

Jacques, S.L., Optical properties of biological tissues: a review. Phys Med Biol, 2013. 58(11):

Intralipid® + india ink



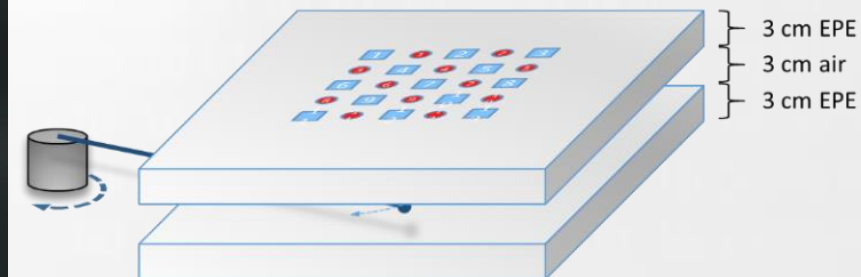
Agar + india ink



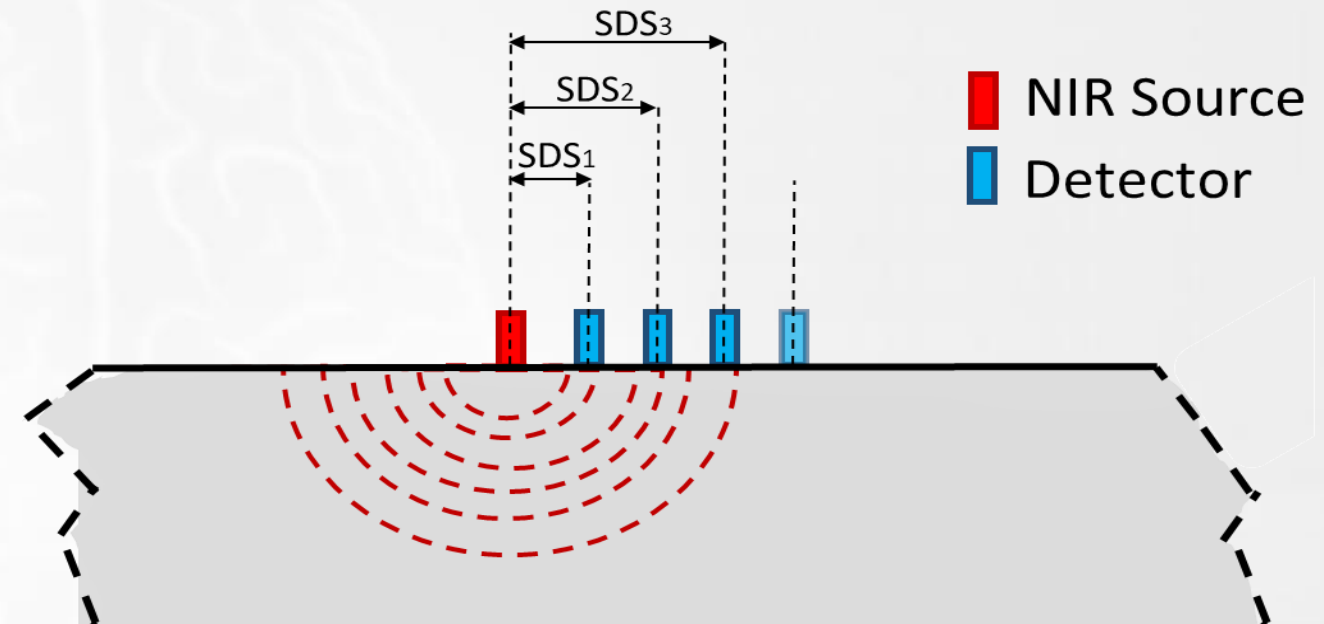
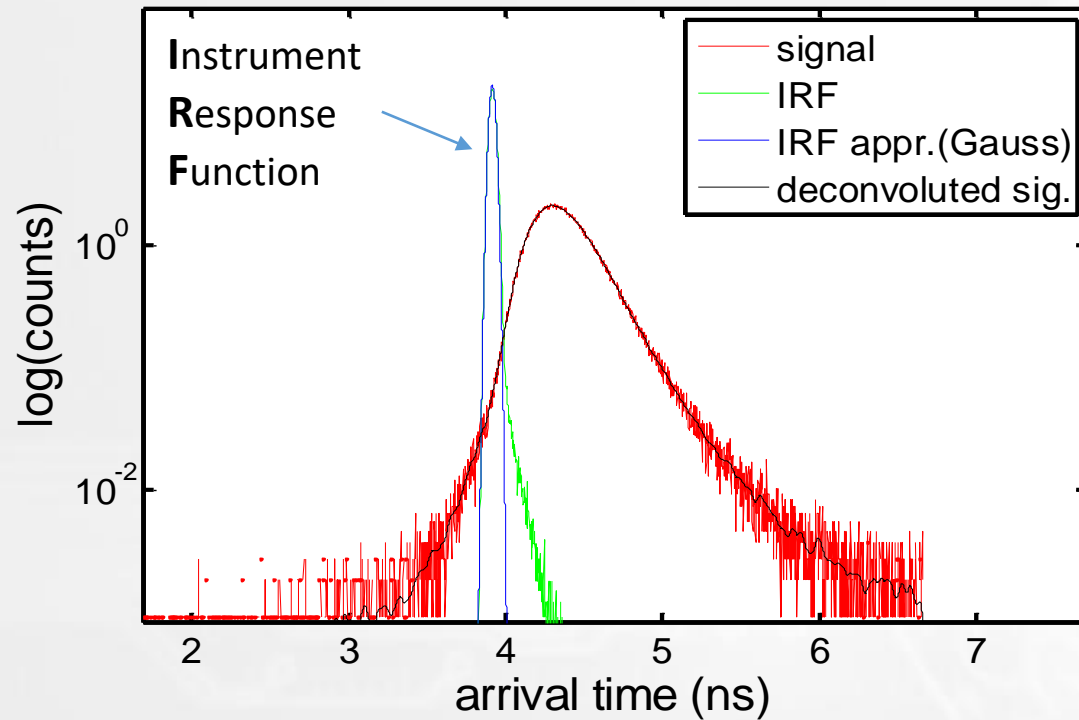
Milk + india ink



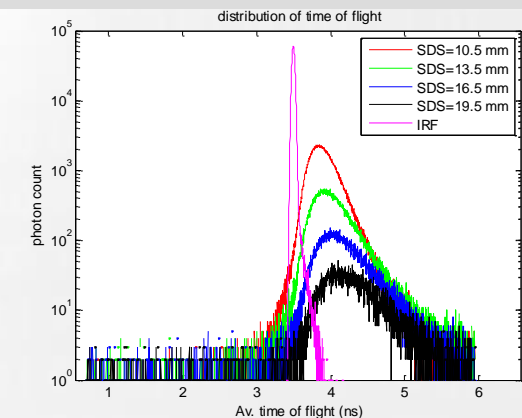
Expanded Polyethylene



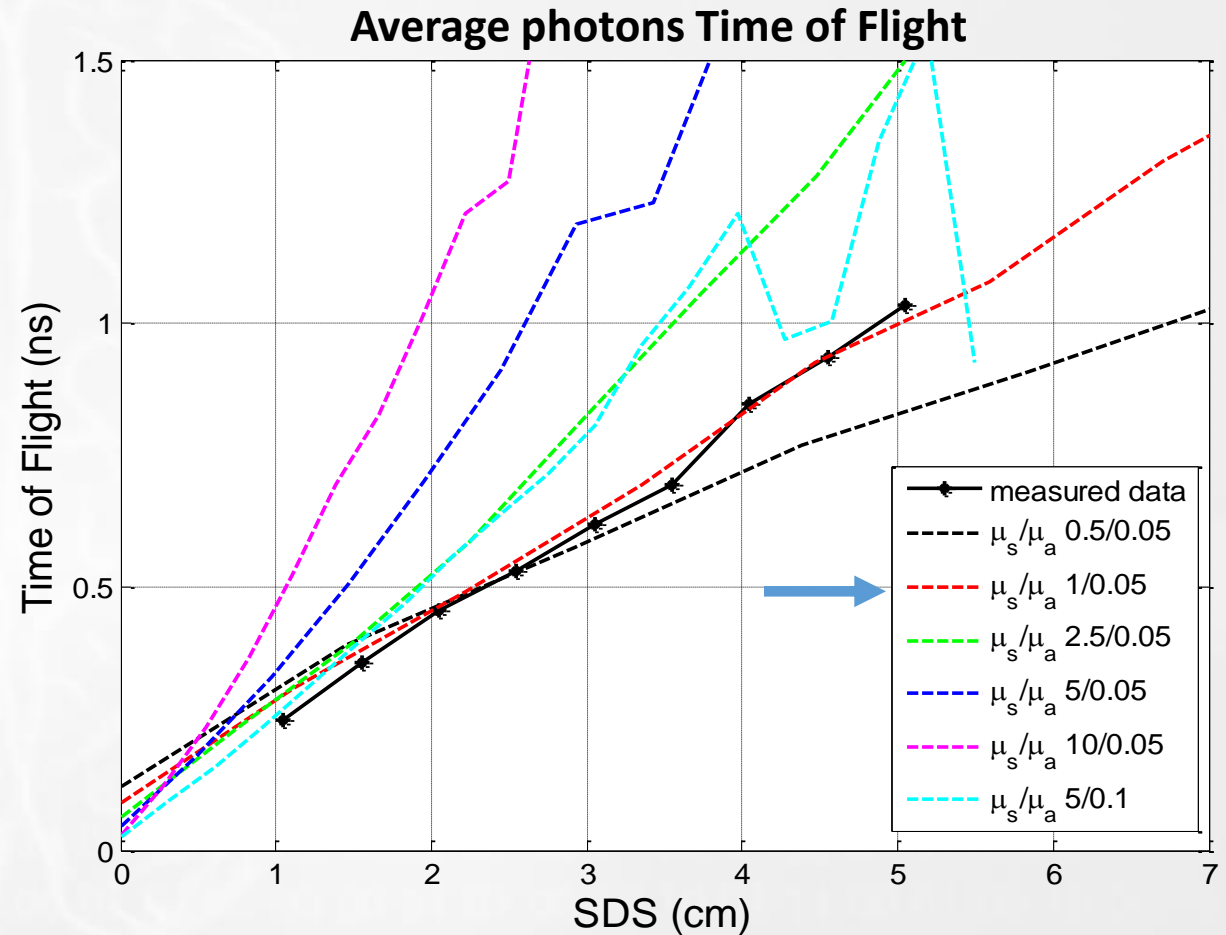
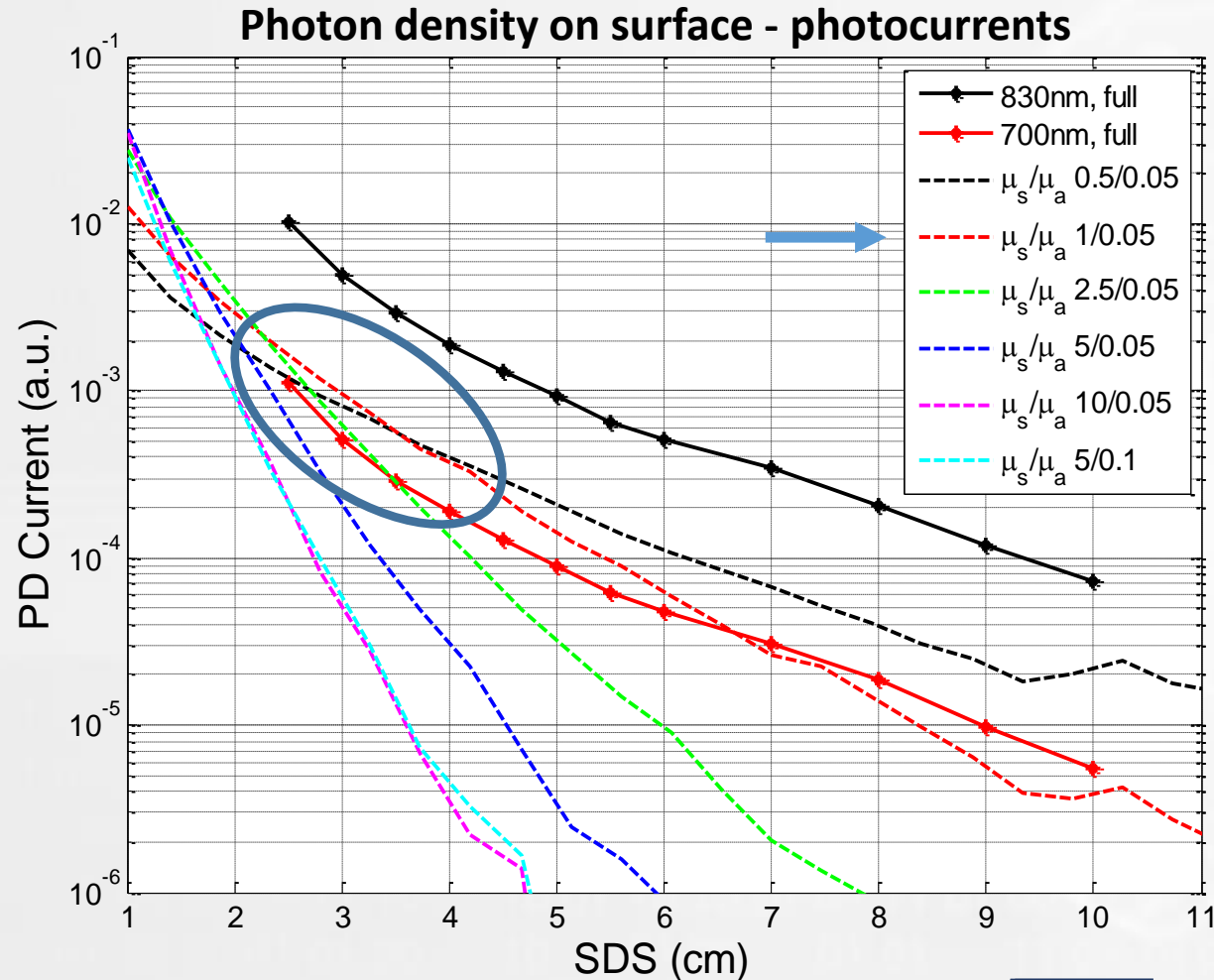
Material optical characterization: Time correlated single photon counting (TCSPC)



Materials optical characterization: Photocurrents + TCSPC + Montecarlo Simulation

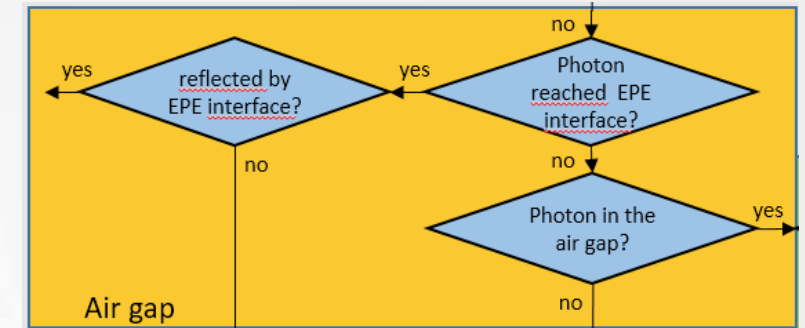
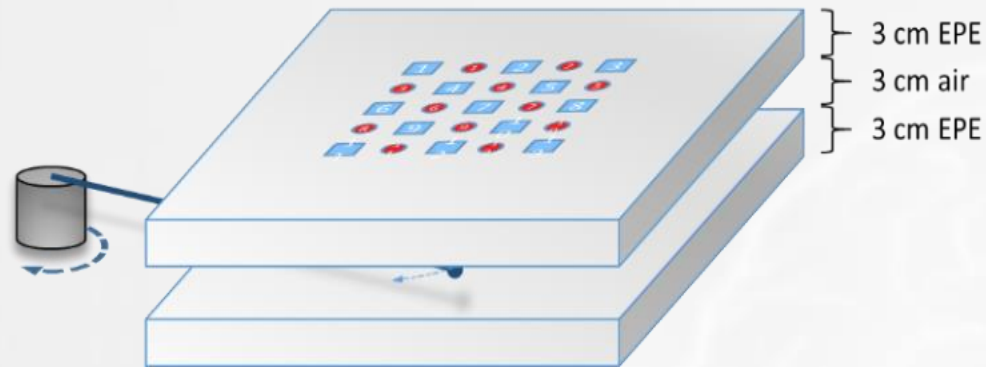


Materials optical characterization: photocurrents + TCSPC + Montecarlo Simulation

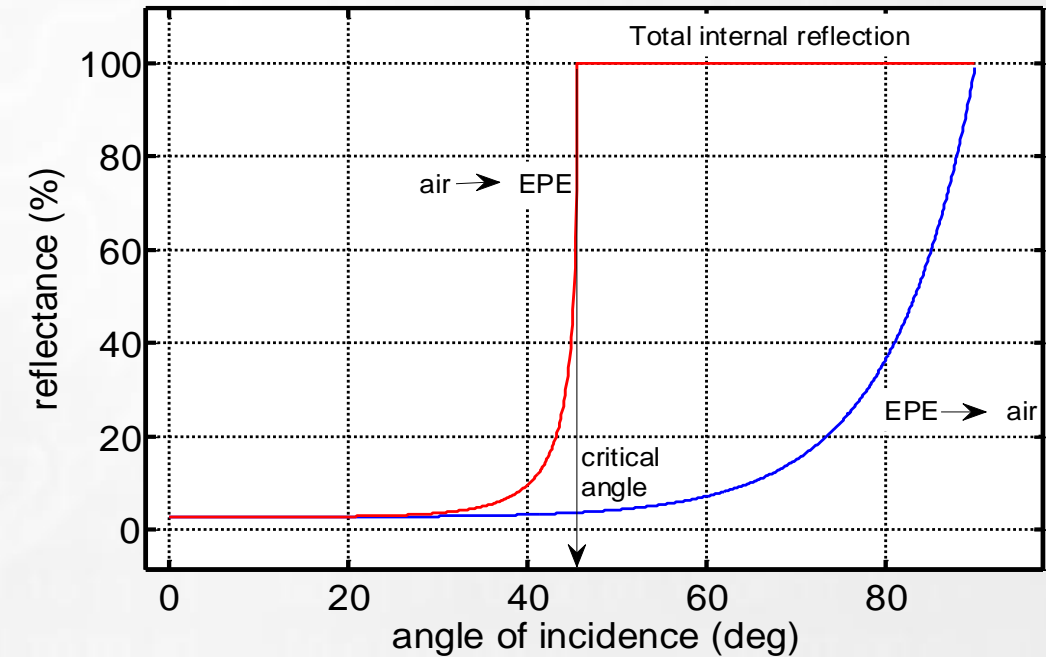
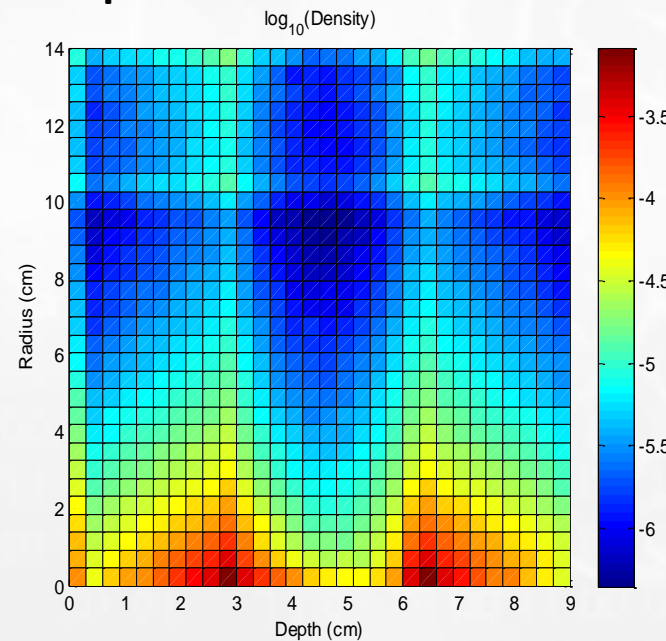
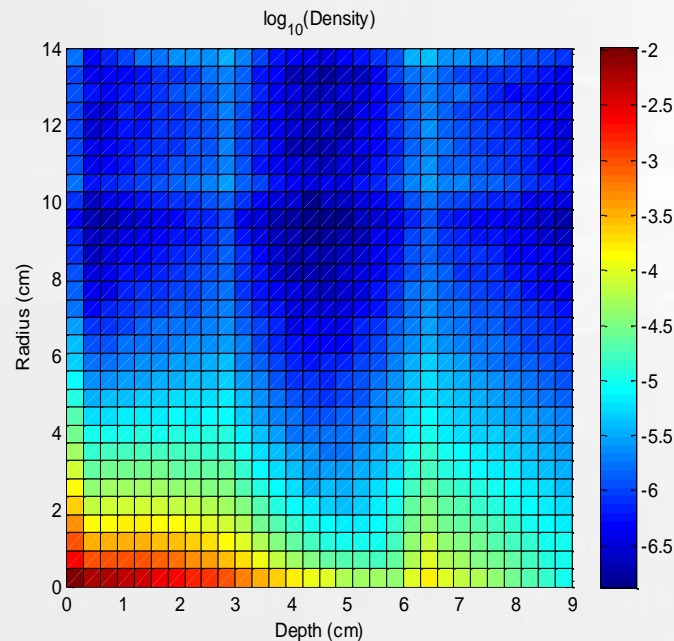


$$\sqrt{\mu_a \cdot \mu'_s} = \sqrt{0.05 \cdot 1} = 0.2 \text{ cm}^{-1}$$

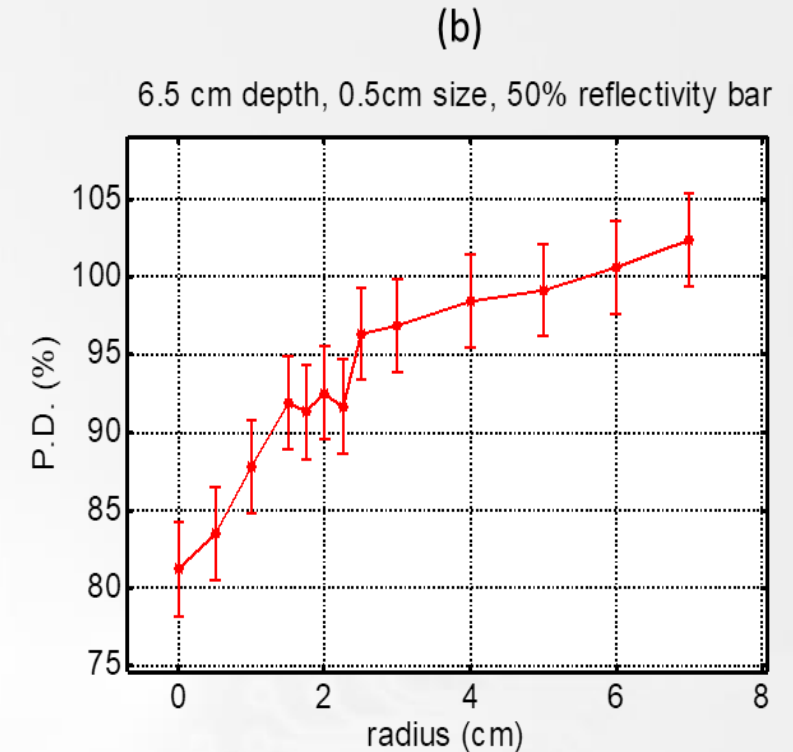
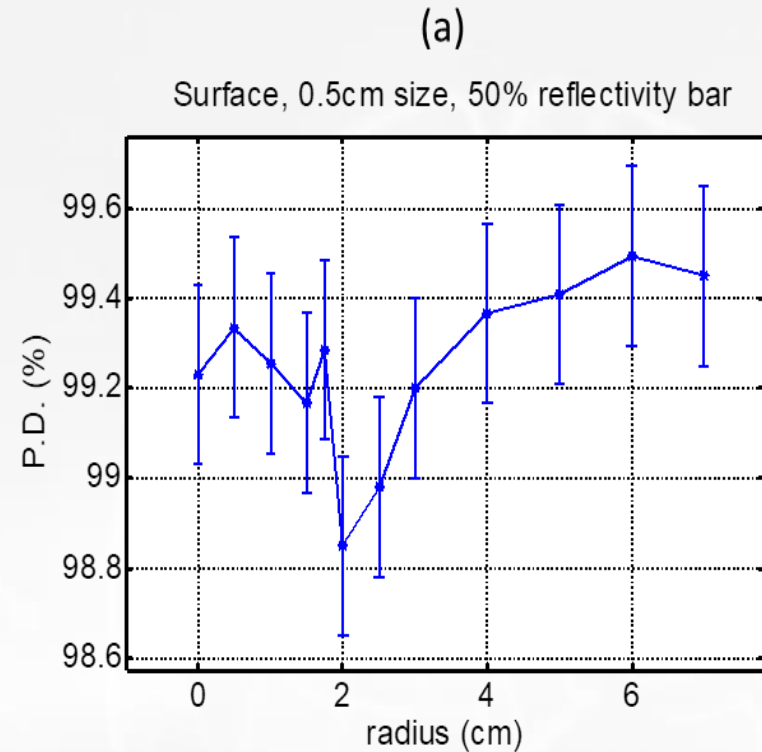
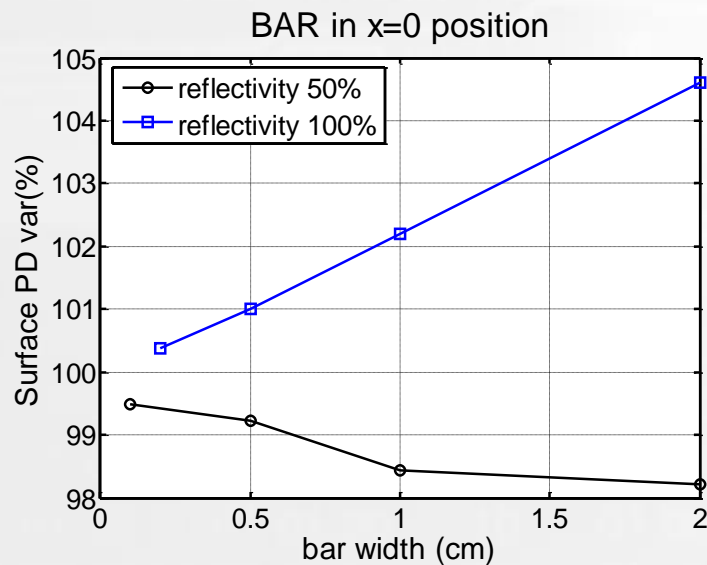
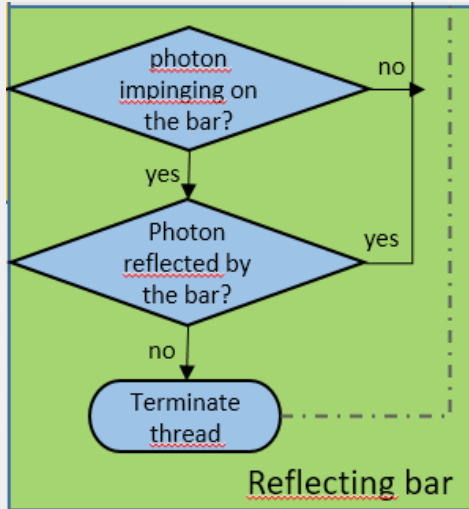
Signals Prediction: Montecarlo Simulation



Montecarlo output



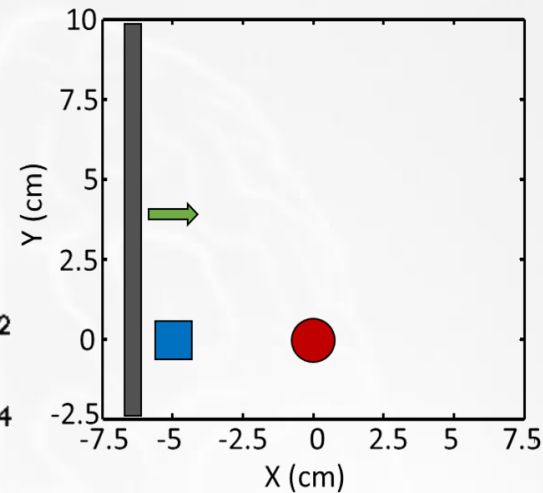
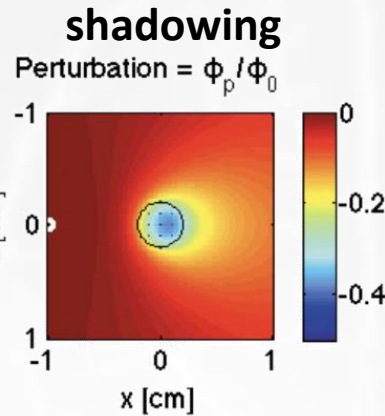
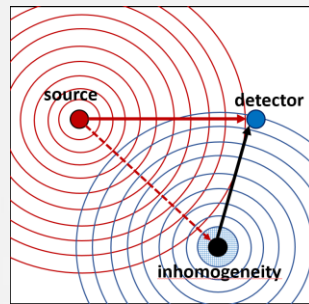
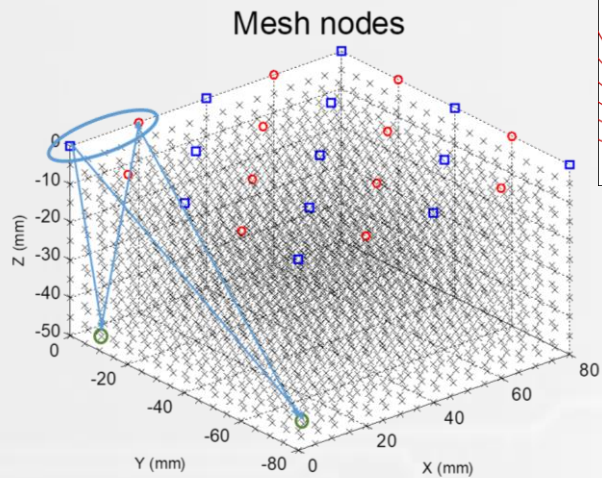
Signals prediction: Montecarlo Simulation



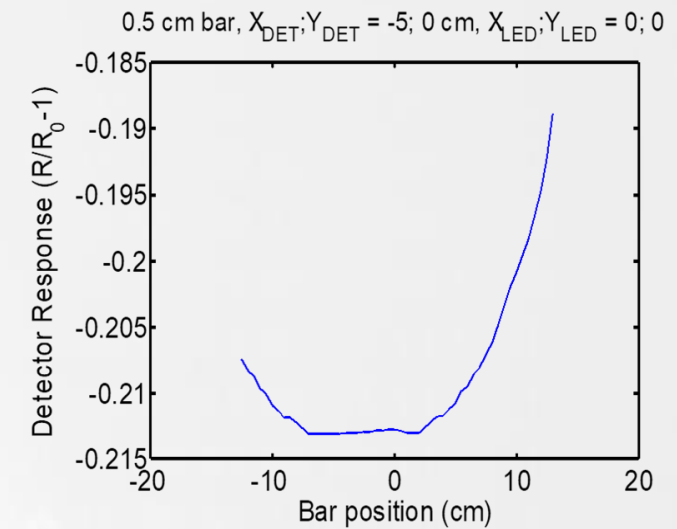
1. Photon density on surface decreases with the bar width (50% reflecting bar in $x = 0$)
2. Photon density on surface has a minimum along the radius

Signals prediction: Montecarlo Simulation

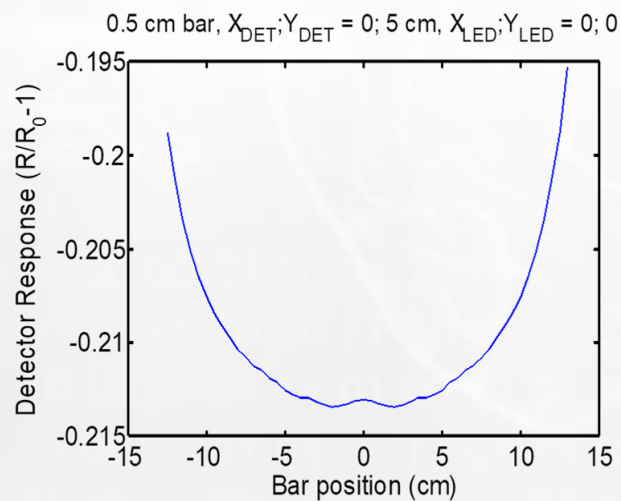
$$y_{sd}(t) \propto \sum_{p=1}^N T_{S \rightarrow v_p}(t) \cdot T_{v_p \rightarrow d}(t)$$



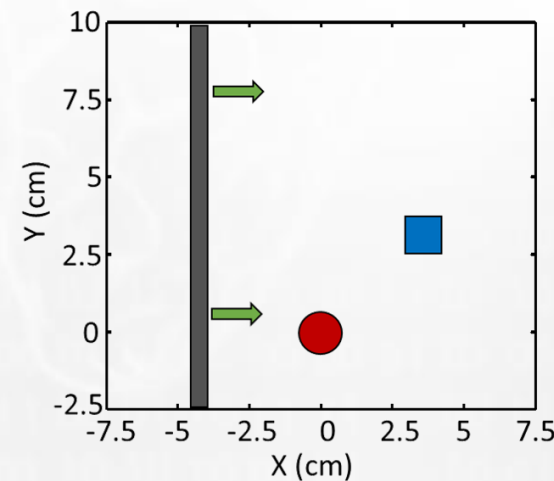
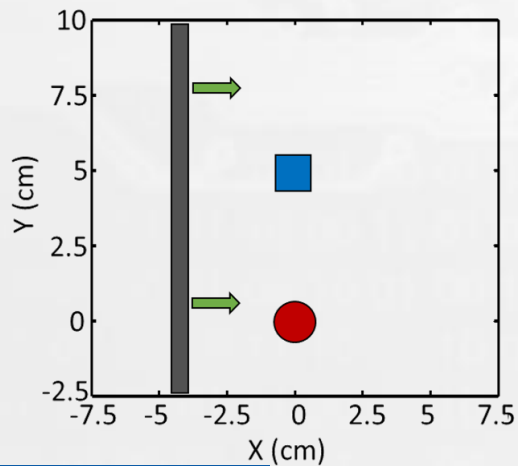
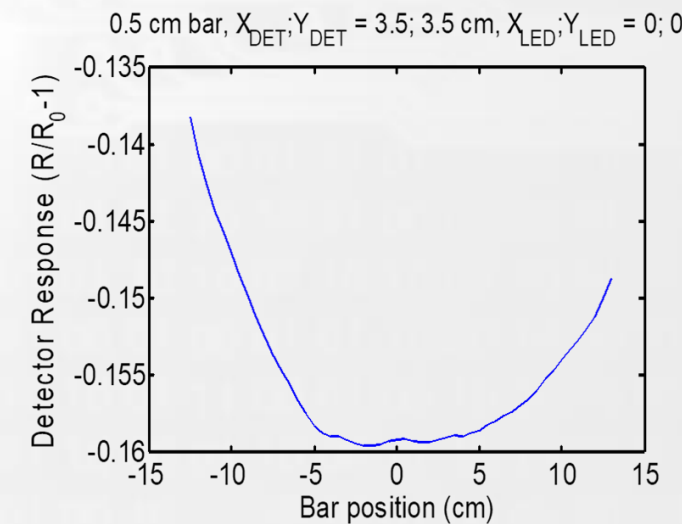
(b)



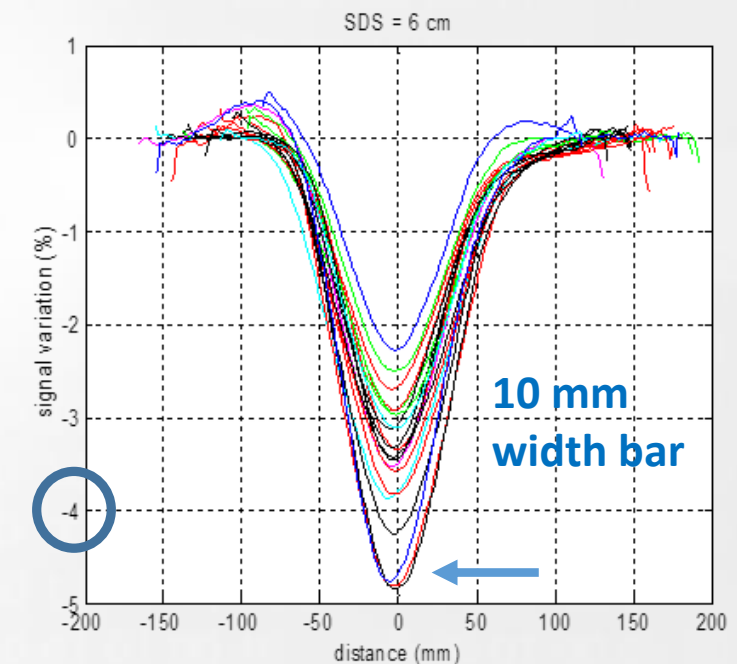
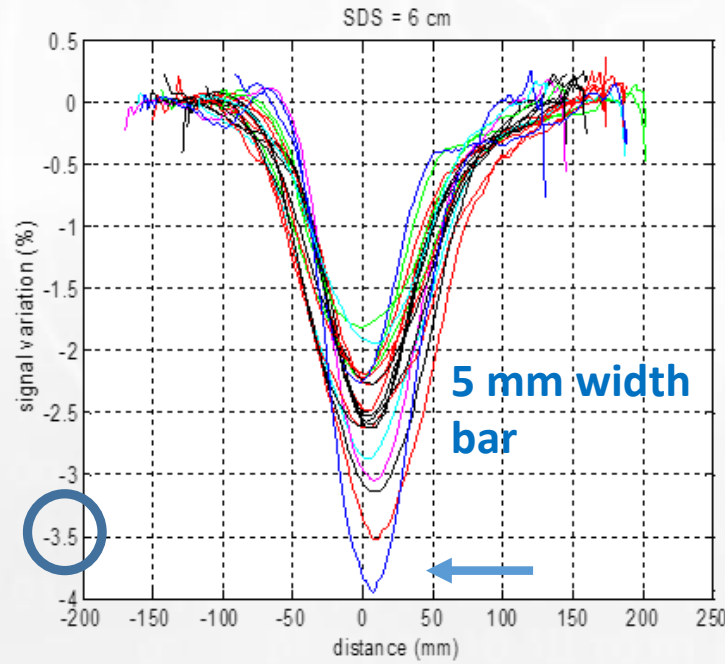
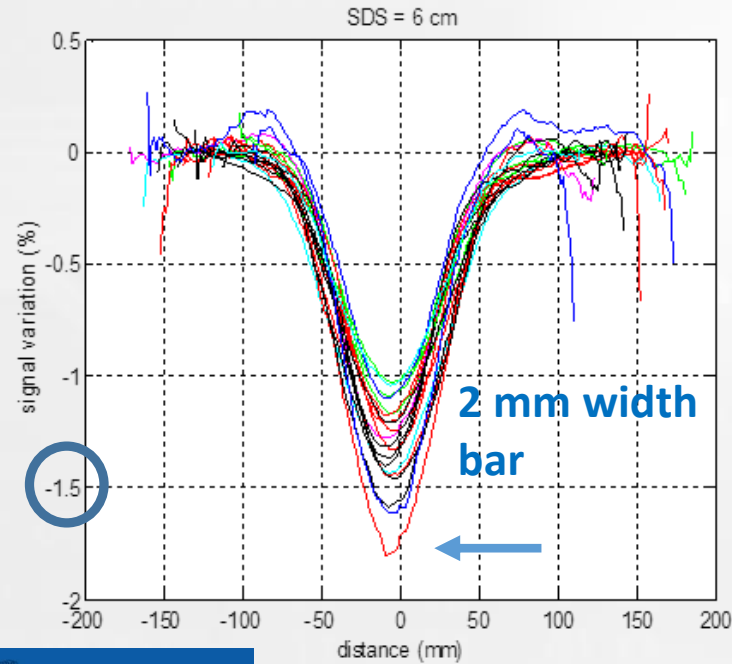
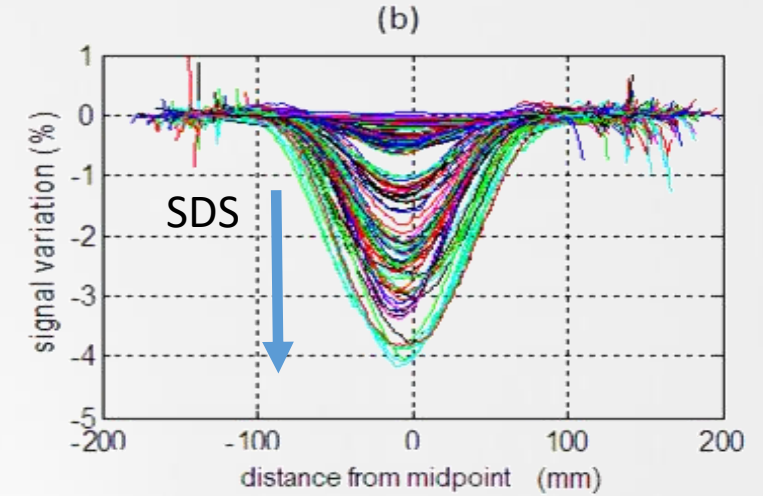
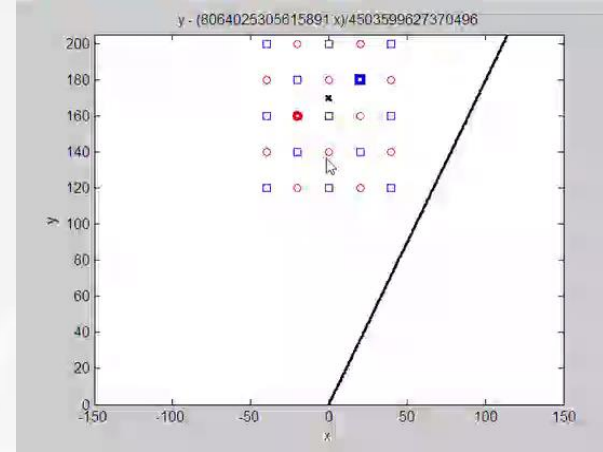
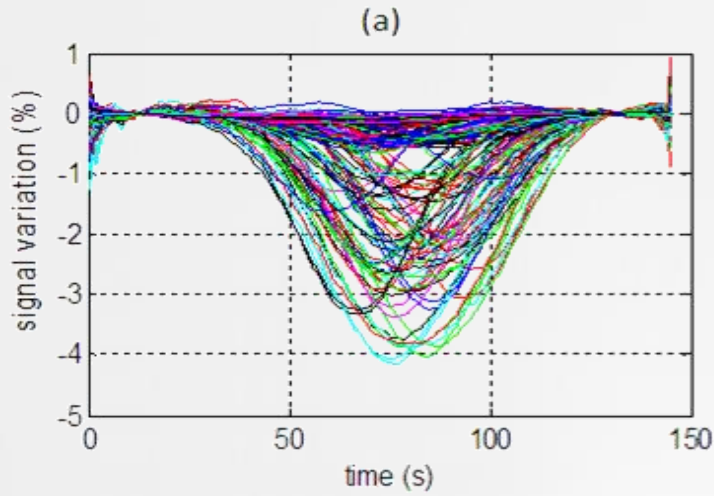
(a)



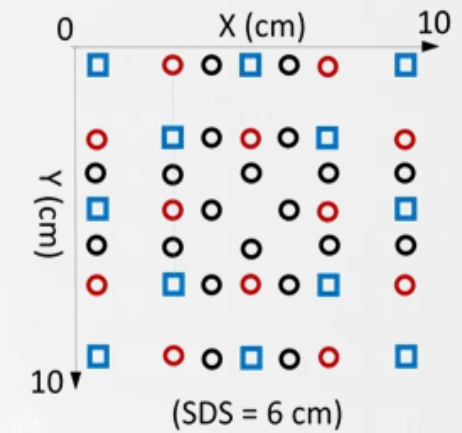
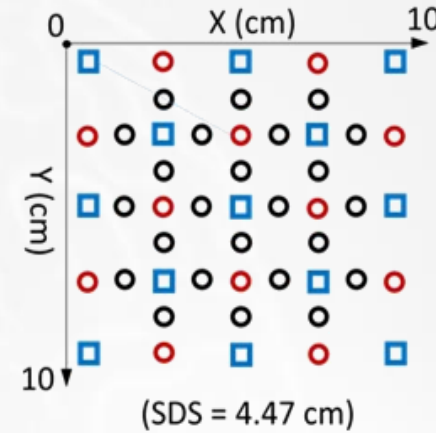
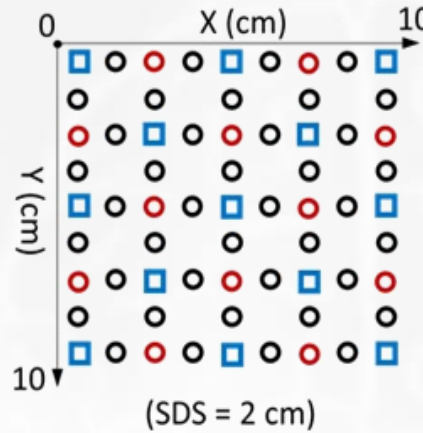
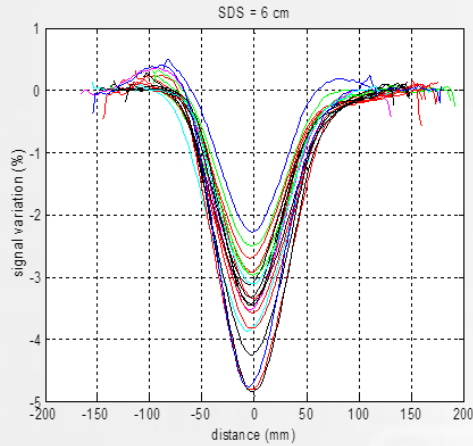
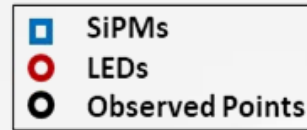
(c)



Signals prediction: Comparison

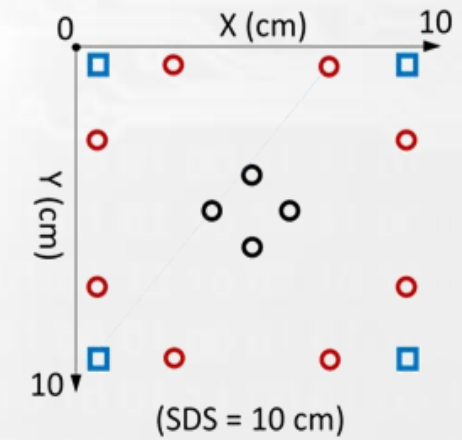
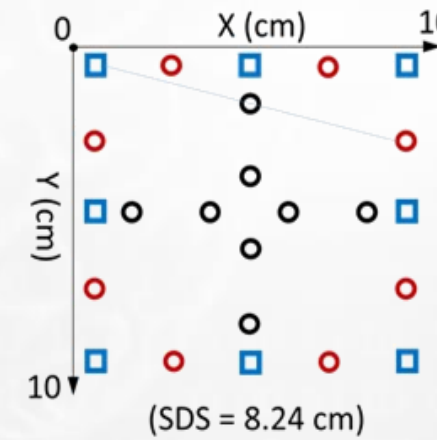
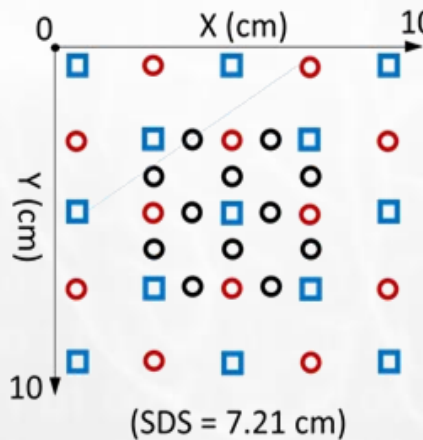


Imaging algorithm for DOT measurements

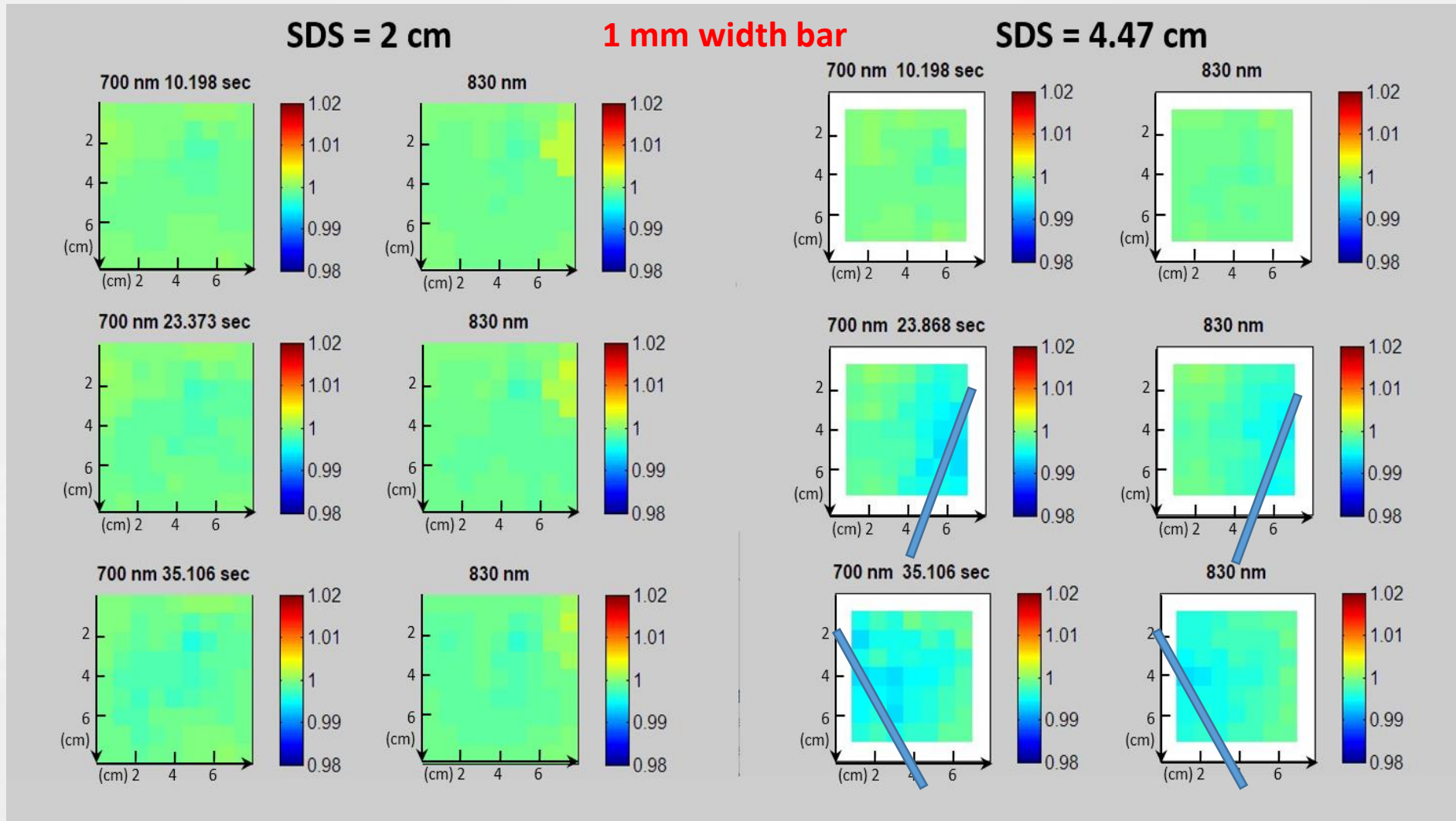


$$D = \sim SDS/2$$

G. Maira, A.M. Chiarelli, S. Brafa, S. Libertino, G. Fallica, A. Merla, S. Lombardo «Imaging system based on Silicon Photomultipliers and Light Emitting diodes for functional Near Infrared Spectroscopy», Applied Sciences (2020)



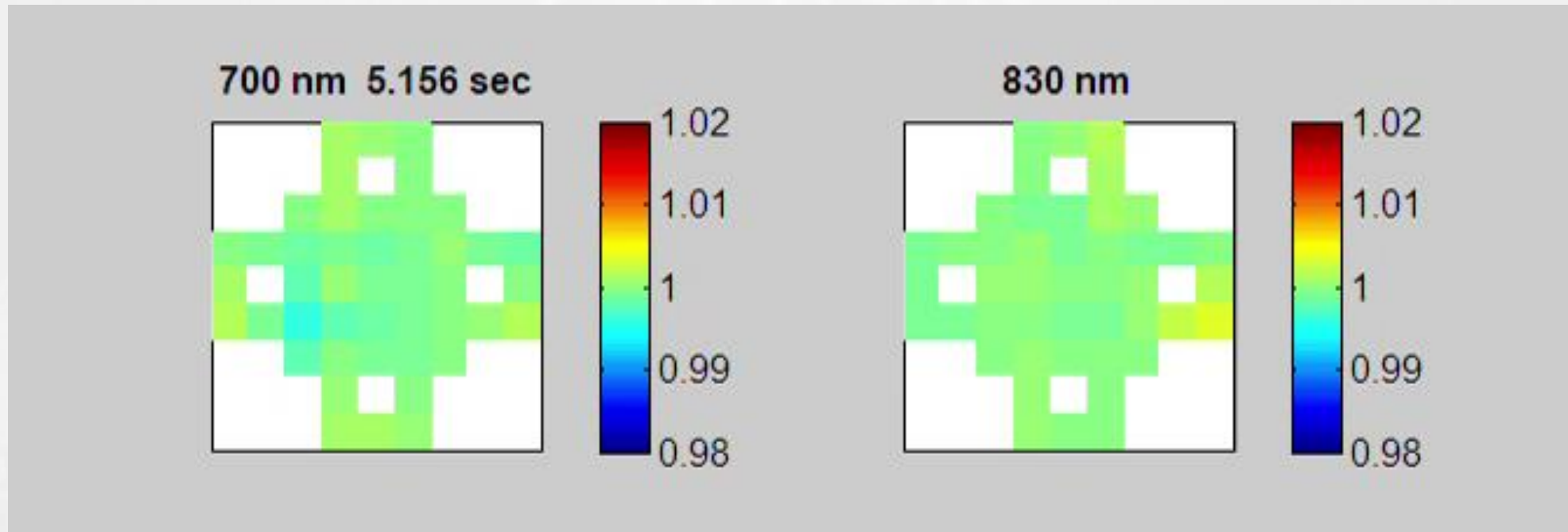
Imaging algorithm for DOT measurements



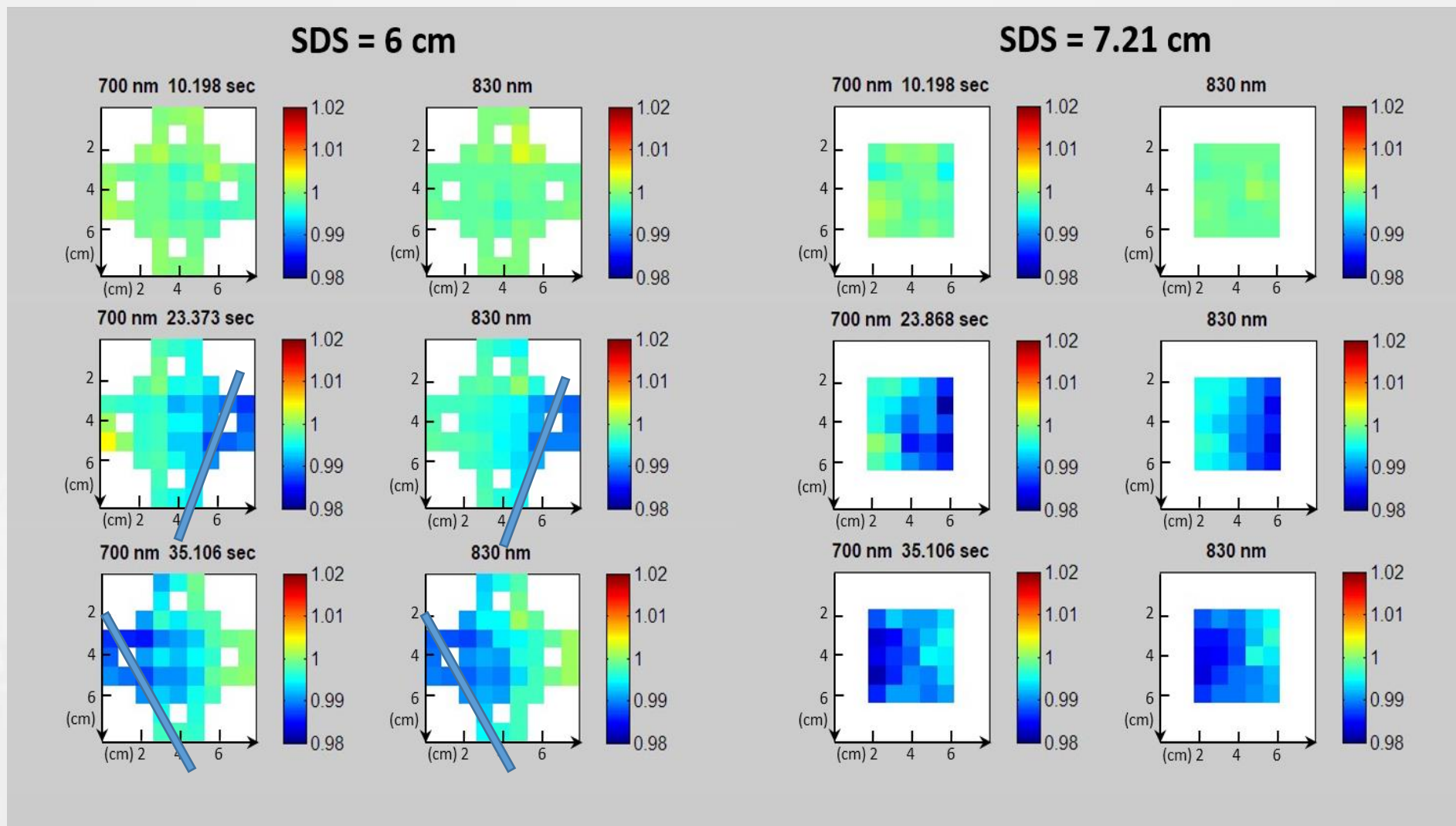
G. Maira, A.M. Chiarelli, S. Brafa, S. Libertino, G. Fallica, A. Merla, S. Lombardo «Imaging system based on Silicon Photomultipliers and Light Emitting diodes for functional Near Infrared Spectroscopy», Applied Sciences (2020)

Imaging algorithm for DOT measurements

SDS = 6 cm , 1 mm width bar

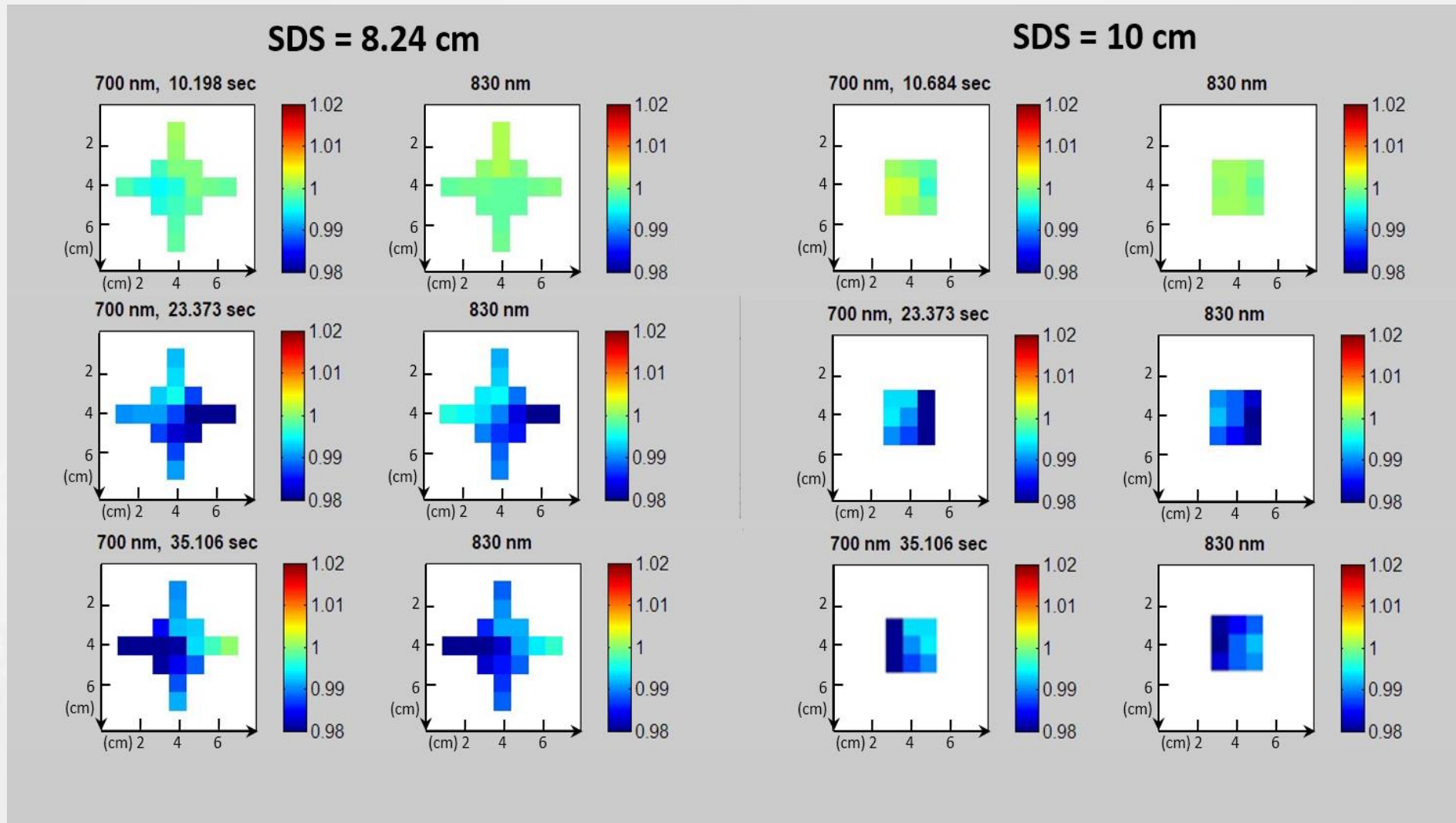


G. Maira, A.M. Chiarelli, S. Brafa, S. Libertino, G. Fallica, A. Merla, S. Lombardo «Imaging system based on Silicon Photomultipliers and Light Emitting diodes for functiona Near Infrared Spectroscopy», Applied Sciences (2020)



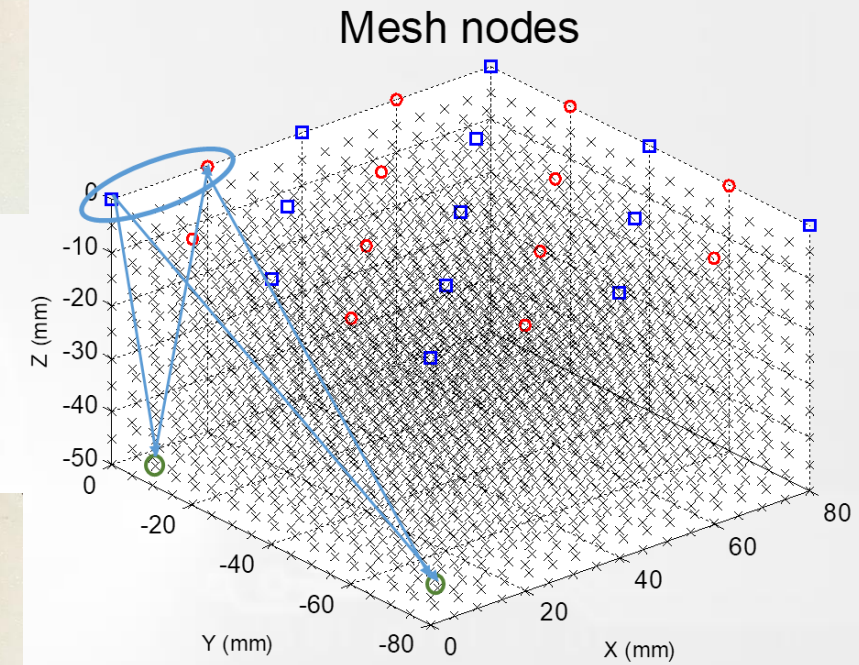
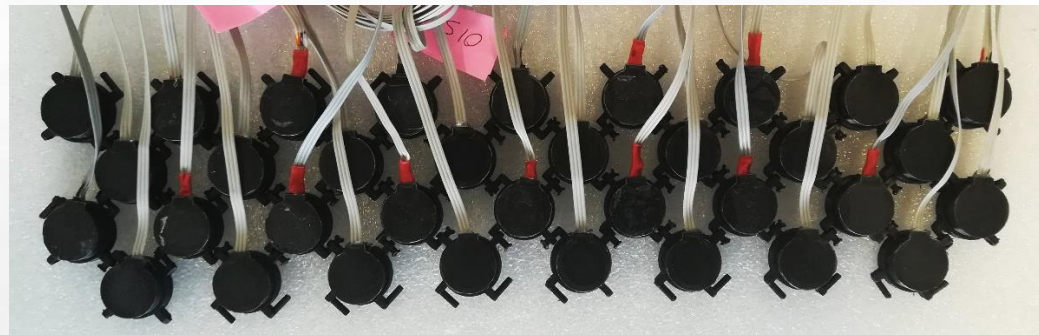
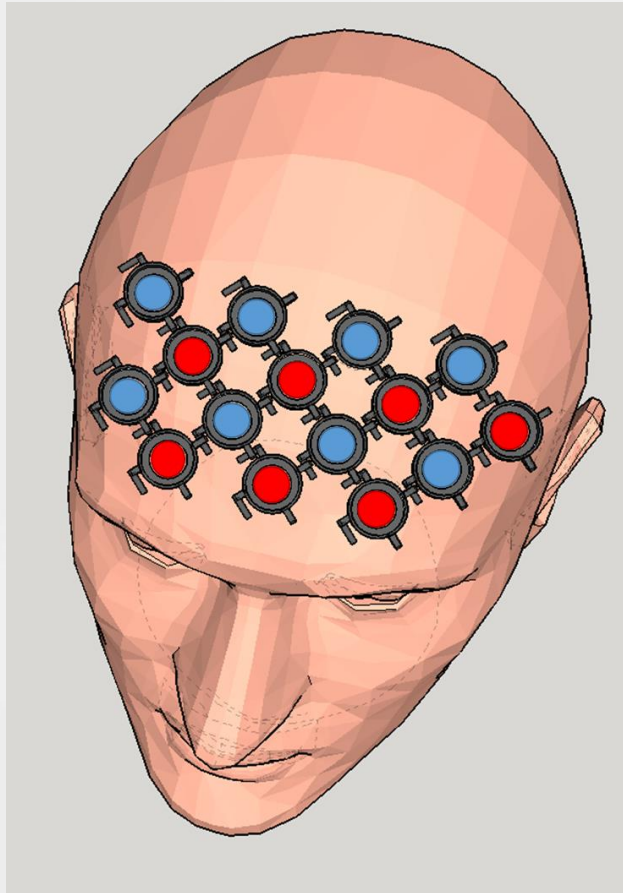
G. Maira, A.M. Chiarelli, S. Brafa, S. Libertino, G. Fallica, A. Merla, S. Lombardo «Imaging system based on Silicon Photomultipliers and Light Emitting diodes for functiona Near Infrared Spectroscopy», Applied Sciences (2020)

Imaging algorithm for DOT measurements



G. Maira, A.M. Chiarelli, S. Brafa, S. Libertino, G. Fallica, A. Merla, S. Lombardo «Imaging system based on Silicon Photomultipliers and Light Emitting diodes for functiona Near Infrared Spectroscopy», Applied Sciences (2020)

Future Work



TOMOGRAPHY

Direct problem:
 $\mathbf{y} = \mathbf{A}\mathbf{x}$

Inverse problem:
 $\hat{\mathbf{x}} = \mathbf{A}^T(\mathbf{A}\mathbf{A}^T + \alpha s_{\max}\mathbf{I})^{-1}\mathbf{y}$

In homogeneous media:

$$a_{i,j} = \frac{\partial}{\partial \mu_{ai}} I_j$$

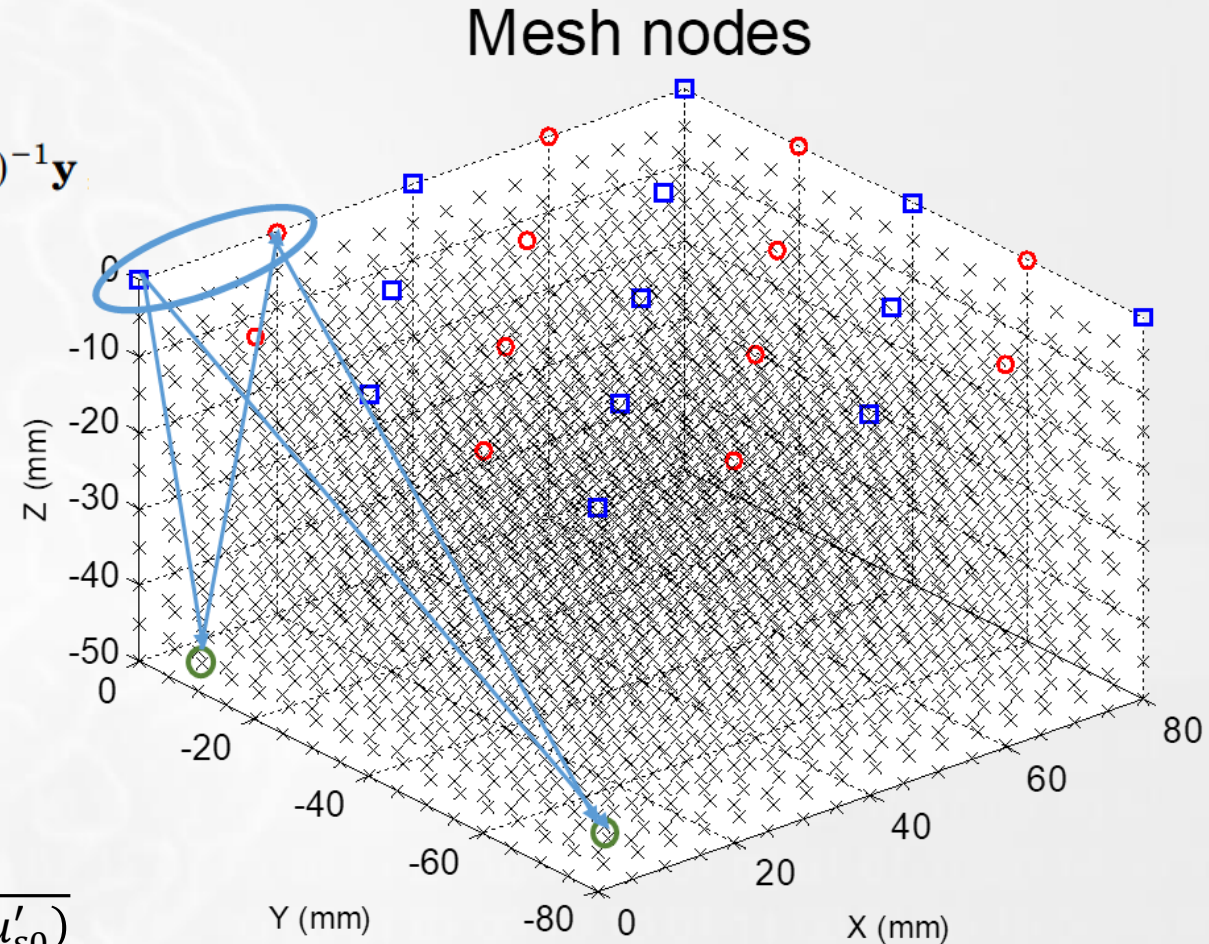
Evaluable with the adjoint method:

$$a_{i,j} = -T_{s \rightarrow p} T_{p \rightarrow d}$$

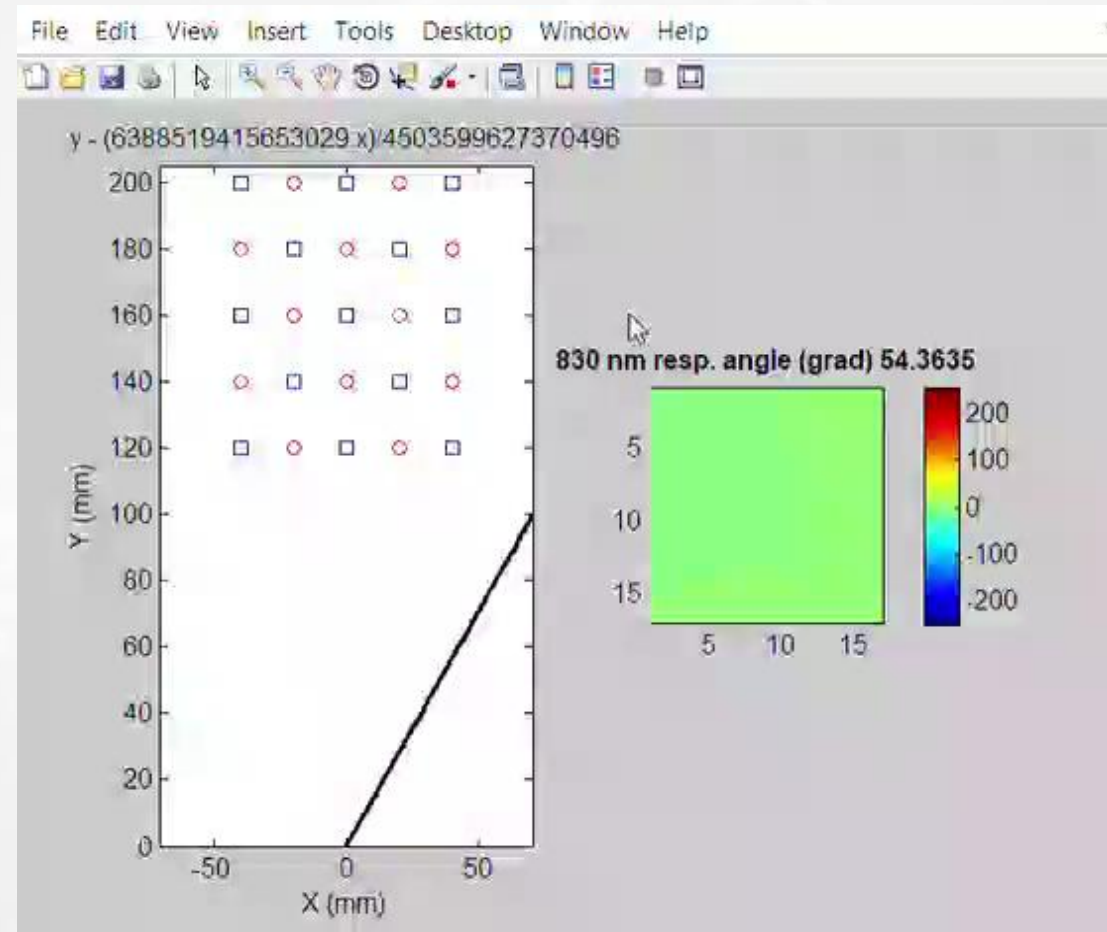
$$T_{s \rightarrow p} = \frac{\exp(-r_{s \rightarrow p}/\delta)}{4\pi D r_{s \rightarrow p}}$$

$$D = \frac{1}{3(\mu_{a0} + \mu'_{s0})}$$

$$\delta = \sqrt{D/\mu_{a0}}$$

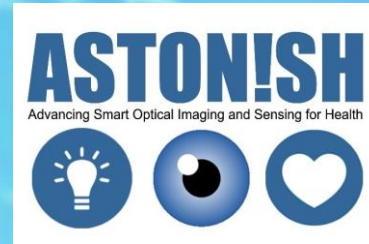


Imaging algorithm for DOT measurements



Conclusions

- **Optimized use of Silicon Photomultiplier devices in fNIRS: Electrical - Physical – Optical Characterization:**
 - After-pulsing
 - Defects
 - Thermal Transients
 - Signal to Noise Ratio optimization
 - Linear range → intellectual property production
- **Realization of an optimized dynamic phantom with light diffusion properties close to human tissues**
- **Baseline optical characterization of materials by Time of flight measurements – Montecarlo simulations**
- **Realization of 156 channels/2 wavelenghts fNIRS/DOT system with optimal use of Si Photomultipliers**
- **Experimental results in excellent agreement with Monte Carlo light diffusion modeling**
- **Imaging algorithm based on back-projection approach**



Thank you!

Gaetano Santoro
Alfredo Ferro

Salvatore Lombardo
Sebania Libertino



Arcangelo Merla
Antonio M. Chiarelli

Giorgio Fallica
Vincenzo Vinciguerra
Delfo Sanfilippo
Massimo Mazzillo

